Taphonomy and taxonomy of a juvenile lambeosaurine (Ornithischia: Hadrosauridae) bonebed from the late Campanian Wapiti Formation of northwestern Alberta Canada

Brayden Holland [Corresp., 1], **Phil R Bell** [1], **Federico Fanti** [2], **Samantha Hamilton** [3], **Derek W Larson** [4], **Robin Sissons** [3], **Corwin Sullivan** [3, 4], **Matthew J Vavrek** [5], **Yanyin Wang** [3], **Nicolás E Campione** [Corresp. 1]

[1] Palaeoscience Research Centre, School of Environmental and Rural Science, University of New England, Armidale, New South Wales, Armidale

[2] Dipartimento di Scienze Biologiche, Geologiche e Ambientali, Alma Mater Studiorum, Università di Bologna, Bologna, Italy

[3] Department of Biological Sciences, University of Alberta, Edmonton, Alberta, Canada

[4] Philip J. Currie Dinosaur Museum, Wembley, Alberta, Canada

[5] Department of Natural History, Royal Ontario Museum, Toronto, Ontario, Canada

Corresponding Authors: Brayden Holland, Nicolás E Campione
Email address: blongle2@myune.edu.au, ncampion@une.edu.au

Hadrosaurid (duck-billed) dinosaur bonebeds are exceedingly prevalent in upper Cretaceous (Campanian-Maastrichtian) strata from the Midwest of North America (especially Alberta Canada, and Montana, U.S.A), but are less frequently documented from more northern regions. The Wapiti Formation (Campanian-Maastrichtian) of northwestern Alberta is a largely untapped resource of terrestrial palaeontological information missing from southern Alberta due to the deposition of the marine Bearpaw Formation. In 2018, the Boreal Alberta Dinosaur Project rediscovered the Spring Creek Bonebed, which had been lost since 2002, along the northern bank of the Wapiti River, southwest of Grande Prairie. Earlier excavations and observations of the Spring Creek Bonebed suggested that the site yielded young hadrosaurines. Continued work in 2018 and 2019 rediscovered ~300 specimens that included a minimum of eight individuals, based on the number of right humeri. The morphology of several recovered cranial elements unequivocally supports lambeoasurine affinities, making the Spring Creek sample the first documented occurrence of lambeosaurines in the Wapiti Formation. The overall size range and histology of the bones found at the site indicate that these animals were uniformly late juveniles, suggesting that age segregation was a life history strategy among hadrosaurids. Given the considerable size attained by the Spring Creek lambeousaurines, it is probable they were segregated from the breeding population during nesting or caring for young, rather than due to different diet and locomotory requirements. Dynamic aspects of life history, such as age segregation, may well have contributed to the highly diverse and cosmopolitan nature of the Late Cretaceous hadrosaurid fauna.

Taphonomy and taxonomy of a juvenile lambeosaurine (Ornithischia: Hadrosauridae) bonebed from the late Campanian Wapiti Formation of northwestern Alberta, Canada

Brayden Holland[1], Phil R. Bell[1], Federico Fanti[2], Samantha Hamilton[3], Derek W. Larson[4], Robin Sissons[3], Corwin Sullivan[3, 4], Matthew J. Vavrek[5], Yanyin Wang[3], Nicolás E. Campione[1]

[1]Palaeoscience Research Centre, School of Environmental and Rural Science, University of New England, Armidale, NSW, Australia

[2] Dipartimento di Scienze Biologiche, Geologiche e Ambientali, Alma Mater Studiorum, Università di Bologna, Bologna, Italy

[3]Department of Biological Sciences, University of Alberta, Edmonton, AB, Canada

[4]Philip J. Currie Dinosaur Museum, Wembley, AB, Canada

[5]Department of Natural History, Royal Ontario Museum, Toronto, ON, Canada

Corresponding Authors:

Brayden Holland and Nicolás E. Campione

University of New England, Armidale, NSW, 2351, Australia

Email address: blongle2@myune.edu.au; ncampion@une.edu.au

Abstract

Hadrosaurid (duck-billed) dinosaur bonebeds are exceedingly prevalent in upper Cretaceous (Campanian–Maastrichtian) strata from the Midwest of North America (especially Alberta, Canada, and Montana, U.S.A), but are less frequently documented from more northern regions. The Wapiti Formation (Campanian–Maastrichtian) of northwestern Alberta is a largely untapped resource of terrestrial palaeontological information missing from southern Alberta due to the deposition of the marine Bearpaw Formation. In 2018, the Boreal Alberta Dinosaur Project rediscovered the Spring Creek Bonebed, which had been lost since 2002, along the northern bank of the Wapiti River, southwest of Grande Prairie. Earlier excavations and observations of the Spring Creek Bonebed suggested that the site yielded young hadrosaurines. Continued work in 2018 and 2019 recovered ~300 specimens that included a minimum of eight individuals, based on the number of right humeri. The morphology of several recovered cranial elements unequivocally supports lambeosaurine affinities, making the Spring Creek sample the first documented occurrence of lambeosaurines in the Wapiti Formation. The overall size range and histology of the bones found at the site indicate that these animals were uniformly late juveniles, suggesting that age segregation was a life history strategy among hadrosaurids. Given the considerable size attained by the Spring Creek lambeosaurines, it is probable they were segregated from the breeding population during nesting or caring for young, rather than due to different diet and locomotory requirements. Dynamic aspects of life history, such as age

segregation, may well have contributed to the highly diverse and cosmopolitan nature of the Late Cretaceous hadrosaurid fauna.

Introduction

Macrofossil bonebeds are a source of palaeontological data that greatly contribute to our understanding of anatomy, diversity, life history, community structure, behaviour, population dynamics, and taphonomy (Rogers et al., 2007). In North America, hadrosaurid dinosaur bonebeds are particularly concentrated in uppermost Cretaceous (Campanian–Maastrichtian) deposits, notably in those of the Belly River and Edmonton groups in southern Alberta, Canada (Getty et al., 1998; Eberth & Getty, 2005; Eberth & Currie, 2010; Bell & Campione, 2014; Eberth, 2015; Evans et al., 2015) and the Two Medicine, Hell Creek, Lance, and Judith River formations in the northern part of the western United States (Christians, 1992; Varricchio & Horner, 1993; Britt et al., 2009; Scherzer & Varricchio, 2010; Keenan & Scannella, 2014; Prieto-Márquez & Gutarra, 2016). Hadrosaurid specimens from bonebeds in these formations were among the first dinosaurs to be histologically sampled, which allowed for the reconstruction of their growth rates (Horner & Currie, 1994) and provided the first evidence for parental care in dinosaurs (Horner & Makela, 1979; Horner et al., 2000). Despite their frequency and importance, there remain large numbers of North American hadrosaurid bonebeds that have not been described in detail, particularly in northern rock units such as the Wapiti Formation (Fanti & Catuneanu, 2009; Fanti & Miyashita, 2009). These offer the opportunity to explore the diversity and preservation of hadrosaurids outside the traditionally sampled North American strata.

The deposits of the Wapiti Formation in northwestern Alberta span the mid-Campanian to upper Maastrichtian and are contemporaneous with most of the Belly River and Edmonton

groups in southern Alberta (Fanti & Catuneanu, 2009; Eberth & Braman, 2012). Unlike its more famous southern counterparts, which are interrupted by marine transgressions of the Bearpaw Formation, the Wapiti Formation is a continuous package of terrestrial sediments (Eberth & Getty, 2005; Fanti & Catuneanu, 2009; Eberth & Braman, 2012). Although the Wapiti Formation was originally well-known only for a single ceratopsian site, the Pipestone Creek Bonebed (Currie et al., 2008a), fieldwork over the past 10–15 years has uncovered abundant vertebrate ichnofossils (Bell et al., 2013; Fanti et al., 2013), articulated skeletons with skin impressions (Bell et al., 2014a; Bell et al., 2014b), microfossil sites (Fanti & Miyashita, 2009), and macrofossil bonebeds (Tanke, 2004; Currie et al., 2008a; Fanti et al., 2015) (Fig. 1).

The Pipestone Creek Bonebed was discovered in 1974 (Tanke, 2004) and has produced disarticulated bones representing at least 27 juvenile- to adult-sized individuals of the ceratopsian *Pachyrhinosaurus lakustai*, along with remains of the dromaeosaurid *Boreonykus certekorum*, tyrannosaurids, and non-dinosaurian vertebrates (Currie et al., 2008a; Bell & Currie, 2016). Its unique faunal content has been used to support hypotheses of dinosaur endemism across Laramidia during the Late Cretaceous (Currie et al., 2008a; Sampson et al., 2010; Lucas et al., 2016). A second major bonebed, the Wapiti River Bonebed, is located west of the Pipestone Creek Bonebed and is dominated by *Pachyrhinosaurus* specimens that have not yet been conclusively identified at the species level. Notably, this bonebed represents one of the most inland occurrences of centrosaurine ceratopsians in North America, given its inferred location relative to the Western Interior Seaway (Fanti et al., 2015). In addition to macrofossil bonebeds (defined as >75% of specimens with a preserved length >5 cm; sensu Eberth et al., 2007a), the Kleskun Hill microfossil site (defined as >75% of specimens with a preserved length <5 cm) preserves a high diversity of vertebrates, including fish, lizards, dinosaurs, and mammals (Fanti

& Miyashita, 2009). Several additional monodominant hadrosaurid bonebeds have subsequently been discovered, although not yet documented in detail (Tanke, 2004; Bell et al., 2014a; Bell et al., 2014b).

The hadrosaurids of the Wapiti Formation are taxonomically enigmatic. *Edmontosaurus regalis* is currently the only species reported from this temporally extensive formation (Bell et al., 2014a; Bell et al., 2014b). The majority of hadrosaurid material so far recovered came from Unit 4 of the formation, which is broadly contemporaneous with portions of the Horseshoe Canyon Formation of southern Alberta, from which *E. regalis* is commonly recovered (Bell et al., 2014a; Bell et al., 2014b; Campione & Evans, 2011; Eberth et al., 2013). Moreover, there is yet to be any definitive evidence to suggest the presence of another hadrosaurid taxon beside *E. regalis* in Unit 4. It is unlikely, however, that *E. regalis* was the only hadrosaurid from the entire formation, given the known diversity of hadrosaurids elsewhere in Alberta and the temporal extent of the Wapiti Formation. For instance, lambeosaurines have yet to be documented from the formation, despite their ubiquity within both the Belly River and Edmonton groups (Lull & Wright, 1942; Evans et al., 2005; Ryan & Evans, 2005; Evans & Reisz, 2007; Evans et al., 2007; Evans, 2010; Brink et al., 2011; Mallon et al., 2012; Eberth et al., 2013; Farke et al., 2013).

In 1988, Grande Prairie Regional College staff discovered several well-preserved hadrosaurid bones along the northern bank of the Wapiti River, approximately 150 m downstream of the confluence with the Spring Creek (Tanke, 2004). The site was dubbed the Spring Creek Bonebed (SCBB), and the material was suggested to possibly pertain to Hadrosaurinae, based on the “low deltoid crests” morphology seen in the recovered humeri. Given their size range, the bones were interpreted as the remains of subadult individuals that may have formed a “bachelor herd” (Tanke, 2004). Initial excavations at the SCBB undertaken by

Grande Prairie Regional College and Royal Tyrrell Museum began in 1988, resulting in a total of 40 specimens recovered between 1988 and 2002. By 2003, however, the site had been obscured by riverbank slumping (Tanke, 2004), and could not be rediscovered despite repeated attempts over the following years. The bonebed was finally rediscovered in 2018 by Matthew Vavrek, as part of the Boreal Alberta Dinosaur Project, and subsequently excavated during the 2018 and 2019 field seasons (Fig. 2). These recent excavations secured hundreds of hadrosaurid specimens, including the first diagnostic cranial material.

In this study, we describe the anatomy of the most taxonomically informative hadrosaurid bones preserved at the SCBB and examine the taphonomic factors that may have formed the bonebed. We test the original suggestion that the material might belong to Hadrosaurinae (Tanke, 2004) using a larger sample that encompasses more diagnostic elements and use histological analyses to assess the age distribution of the bonebed sample. Finally, we consider the nature of fossil deposition at the SCBB, with a particular focus on whether the bonebed assemblage originated through attrition or mass mortality, and explore the implications for how hadrosaurid life histories should be envisaged.

Geological setting

Outcrops of the terrestrial Wapiti Formation are exposed extensively in the central to northwestern regions of Alberta (Fig. 1) and into the eastern-most regions of British Columbia. Stratigraphically, the Wapiti Formation overlies the marine Puskwaskau Formation and underlies the terrestrial Scollard Formation (Fanti & Catuneanu, 2009). Spanning from the mid-Campanian (~79.1 Ma) into the Maastrichtian (~67 Ma), the Wapiti Formation is roughly contemporaneous

with the Belly River and Edmonton groups of southern Alberta, and the Two Medicine and St. Mary River formations of northwestern Montana (Fanti & Catuneanu, 2010; Eberth & Kamo, 2020). The formation is subdivided into five units that suggest an overall progression from channel-fill sandstones to floodplain-derived finer sediments (Fanti & Catuneanu, 2009, 2010). Importantly, coals from Unit 3 and the Red Willow coal zone (upper Unit 4) are interpreted as synchronous with the maximum flooding surfaces of the marine Bearpaw Formation and Drumheller Marine Tongue, respectively (Fanti & Catuneanu, 2009). However, actual marine sediments do not interrupt the succession of terrestrial strata in this region, as they do in southern Alberta. Therefore, the Wapiti Formation represents a nearly continuous mid-Campanian–Maastrichtian terrestrial record that is important for tracking faunal transformation in northern Laramidia, particularly during times when marine transgressions inundated southern Alberta.

Because the Wapiti Formation exposures in which the SCBB is located are highly unstable and prone to slumping, the stratigraphic position of the bonebed can only be confidently determined to within a few metres. The SCBB is located ~11.5 km downstream of the Pipestone Creek Bonebed, placing it within Unit 3 of the Wapiti Formation and implying rough contemporaneity with the lowermost units of the Horseshoe Canyon Formation (the Strathmore and Drumheller members: Currie et al., 2008b; Eberth & Braman, 2012). Unit 3 comprises channel sandstones overlain by interbedded mudstones and siltstones, minor sandstone sheets, and extensive coals, representing fluvial point bars within high-sinuosity fluvial systems in floodplain environments (Fanti & Catuneanu, 2009). At the SCBB locality (Fig.), approximately 14 vertical metres of the Wapiti Formation are exposed on a cutbank of the Wapiti River where slumping has obscured some sedimentary features and the boundaries between horizons. Nevertheless, massive mudstones up to 5.5 m thick (interrupted by thin sandy layers) dominate

the exposure, alternating with sandstones up to 2.8 m thick (Fig. 3). The SCBB is confined to a ~40 cm thick horizon within the middle of a massive, organic-rich mudstone approximately 3.7 m thick. Bones exhibit no signs of grading, range from 10 to 640 mm in maximum length, and have no distinct preferred orientation (see Results). In addition to bones, coalified plant remains (< 10 cm), clay nodules, and amber (< 2 cm) are also present in the bonebed. Conformably underlying the bonebed-hosting mudstone is a ~80 cm thick sandstone with shallow crossbedding, which in turn overlies a coal layer that is only exposed during periods of low water. The overall sedimentary evidence indicates the SCBB was deposited on a vegetated floodplain traversed by the meandering rivers that were the main depositional environment for Unit 3 (Fanti & Catuneanu, 2009).

Materials & Methods

Excavation

Specimens collected by the Grande Prairie Regional College in 1988 and 1991 were mapped but could not be placed in our quarry maps or used in our quarry analyses because accompanying orientation data, field identifications and field numbers were not recorded. During the Boreal Alberta Dinosaur Project excavations in 2018 and 2019, orientation, plunge, and maximum preserved length were recorded on-site for all specimens with a length:width ratio ≥ 2. Obvious taphonomic artefacts, such as fracturing, were noted. All specimens with a total length > 5 cm were mapped by hand in 1 x 1 m grids, subdivided into 10 x 10 cm squares. Specimens collected in 1988 and 1991 are accessioned at the Royal Tyrrell Museum of Palaeontology (TMP), Drumheller, Alberta, Canada (TMP1988.094 and TMP1991.137 series), whereas

specimens collected in 2018 and 2019 are accessioned in the collections of the University of Alberta's Laboratory for Vertebrate Palaeontology (UALVP), Edmonton, Alberta, Canada.

Histology

For consistency, we followed the methods and definitions used in previous histological studies of hadrosaurids (Horner et al., 1999; Horner et al., 2000; Vanderven et al., 2014; Woodward et al., 2015). As humeri were the most abundant element type in the sample (n = 13), they were chosen for histological analysis to determine the age(s) of the individuals to which they belonged (Fig. 4; Table 1). All specimens were sectioned at the mid-diaphysis. Thin sections of TMP specimens were produced at the University of New England (Australia), and thin sections of UALVP specimens were produced at the University of Alberta (Canada).

Humeri sectioned at the University of New England were partially encased in epoxy resin to minimize damage during sectioning. The sections were cut using a diamond saw, before being mounted to slides and hand-polished with 600 grit silicon carbide. Slides were then placed into a Petrothin thin sectioning machine and ground down to 200 μm. The slides were then placed into a Logitech LP50 polisher to be ground down to 30 μm. Sections were analyzed under 10X magnification on a Leica DM500 compound microscope. No images were captured of these sections.

Humeri prepared at the University of Alberta were sectioned at mid-diaphysis using a table saw. Sections were then placed into plastic containers before being covered by EAGER Polymers' EP4101UV Crystal Clear Polyester Resin (Castolite AP & Castolite AC) and EP4920 MEK-P Castolite Hardener (mixed in a 1 oz: 10 drops volume ratio). The cured resin blocks

198 were cut in half using a table saw and mounted on plexiglass slides. Prior to mounting, both the
199 plexiglass slides and resin blocks were faced using 1000 grit silicon carbide grinding mixture.
200 The sections were then ground down on a Hillquist saw using 600 and 1000 grit grinding
201 mixtures until suitable transparency, rather than any predefined thickness, was achieved. Images
202 were captured under 4X magnification using a Nikon DS-FI3 camera, mounted on a Nikon
203 Eclipse E600 POL microscope, and Nikon NIS Elements (v. 4.60) imaging software housed in
204 the Caldwell Lab, University of Alberta.

205

206 Taphonomy

207 All specimens were identified and inspected for taphonomic and preparation artefacts following
208 laboratory preparation. Taphonomic analyses follow the procedures outlined by Behrensmeyer
209 (1991) and built upon by Eberth et al. (2007a) and Blob and Badgley (2007). Taphonomic
210 parameters were broadly categorized into either assemblage, quarry, or bone modification data,
211 and analyzed under subcategories as outlined by Behrensmeyer (1991). In this study, a specimen
212 is defined as a vertebrate hard part (e.g., bone, tooth, scale) regardless of possible association
213 with another bone (Blob & Badgley, 2007). Accordingly, multiple fused bones represent a single
214 specimen, whereas unfused, but associated, bones (e.g., a string of vertebrae) are counted
215 individually as distinct specimens. An element is defined as a vertebrate hard part in its entirety,
216 such as a complete tibia as opposed to a distal piece of a tibia (Badgley, 1986; Blob & Badgley,
217 2007). A broken, but matchable element (e.g. a femur broken into four pieces, or distal and
218 proximal ends of a femur) is regarded as a single specimen if the pieces can be reassembled.
219 Analyses of taphonomic data utilized the total number of specimens (N), the number of
220 identifiable specimens (NISP), and the number of prepared specimens (NPSP). The NISP is

larger than the NPSP because few prepared specimens could not be identified. Except where noted, bone modification data are based on the NPSP, whereas assemblage and quarry data are based on the NISP. The minimum number of individuals (MNI) was determined by counting the most common unique skeletal elements (Blob & Badgley, 2007), which in the case of the SCBB were right humeri (Fig. 3; Table 1).

Voorhies (1969) groups are commonly used to assess skeletal representation and fluvial influence in bonebeds (Gangloff & Fiorillo, 2010; Bell & Campione, 2014; Evans et al., 2015). However, their application to large-bodied extinct taxa has been questioned (Eberth et al., 2007a; Britt et al., 2009; Peterson et al., 2013), as Voorhies groups do not account for bone completeness and disarticulation, particularly of the skull, prior to transportation. Additionally, Voorhies groups were originally used to examine the taphonomy of skeletally fused mammals rather than reptiles. Such factors can cause inaccurate element counts, leading to incorrect ratios between Voorhies groups and false inferences regarding fluvial influence, but elements can be counted more accurately by accounting for the lack of skeletal fusion in younger hadrosaurids (Horner & Currie, 1994). Moreover, the relative proportion of element representation is more informative than absolute counts (Gangloff & Fiorillo, 2010; Bell & Campione, 2014). For this study, Voorhies groups are based on inferred susceptibility to transport given a specimen's size (as redefined by Scherzer & Varricchio, 2010; Varricchio, 1995) and the expected numbers of each element in a single hadrosaurid skeleton were derived from Horner et al. (2004) and Bell and Campione (2014) (Table 3).

243 ## Results

244 Anatomical descriptions

245 The most diagnostic elements recovered from the SCBB include a premaxilla, maxilla,
246 and postorbital, all of which show unambiguous lambeosaurine affinities. These elements are
247 described in detail below.

248 *Premaxilla*—A partial left premaxilla (UALVP 60537) is preserved in two equal-length
249 but non-contiguous pieces, separated by a gap of several millimetres (Fig. 5). Most of the
250 anterior region of the premaxilla is intact, revealing the facial angle and the shape of the bill.
251 However, the posterior contact with the nasal is absent, as is most of the premaxillary
252 contribution to the cranial crest.

253 The oral margin of the premaxilla is rugose and was likely covered by a keratinous
254 rhamphotheca in life (Morris, 1970; Horner et al., 2004; Farke et al., 2013). In dorsal view, the
255 oral margin is transverse anteriorly and broadly arcuate more posteriorly with a smooth transition
256 to the post-oral region of the premaxilla. As a result, it does not form a distinct, ventrolaterally
257 directed tab-like process, as seen in other juvenile lambeosaurines (such as *Hypacrosaurus*,
258 *Parasaurolophus*, and *Velafrons coahuilensis*), although the extent of this process varies with
259 ontogeny (Gates et al., 2007; Evans, 2010; Brink et al., 2011; Farke et al., 2013). The anterior
260 third of the preserved length of the premaxilla's dorsal surface is concave mediolaterally,
261 corresponding to the contour of the bony naris. The preserved bony naris has a length:width ratio
262 of 3.5, exceeding the ratio observed in the southern Laramidian taxa *Magnapaulia laticaudus*
263 and *V. coahuilensis* (1.85–2.85; Prieto-Márquez et al., 2012), though this is likely due to
264 ontogeny (Prieto-Márquez et al., 2012). The bony naris attenuates anterior to the crest-snout

265 angle, similar to juvenile *Lambeosaurus lambei* and *Hypacrosaurus altispinus* (Lull & Wright,
266 1942; Ostrom, 1961; Evans et al., 2005; Evans, 2010), but in contrast to the more posterior
267 attenuated bony naris seen in juvenile *Corythosaurus* (Evans et al., 2005; Evans, 2010).

268 The posterolateral process is missing, exposing part of the narial vestibule in lateral view.
269 In lateral aspect, the posterodorsal process becomes more dorsally inclined posteriorly, in the
270 region representing the anterior part of the base of the crest. As preserved, the posterolateral
271 process suggests a crest-snout angle of ~158°, which is more consistent with the range identified
272 for *H. altispinus* (140°–163°), than those for other lambeosaurines (*Lambeosaurus*: 62–153°;
273 *Corythosaurus*: 116–155°; *Hypacrosaurus stebingeri*: 140°–152°; Evans, 2010; Brink et al.,
274 2014).

275 *Maxilla*—The right maxilla (UALVP 59881b) retains the typical triangular body seen in
276 all hadrosaurids (Horner et al., 2004; Evans, 2010; Brink et al., 2011), despite lacking most of
277 the dorsal process and roughly half of the maxillary body anterior to the dorsal process (Fig. 6).
278 The anterior fracture represents a dorsoventral shear revealing a cross-section of the most
279 anteriorly preserved maxillary tooth family, showing at least three replacement teeth enclosed
280 within the maxillary body. In dorsal view, a shelf that would have supported the posterolateral
281 process of the premaxilla extends medially from the maxillary body (Horner et al., 2004). Lateral
282 to the medial shelf is a large oblate foramen that opens along the anterodorsal margin of the
283 dorsal process; the presence of a foramen at this location is characteristic of lambeosaurines
284 (Horner et al., 2004). Lateral to the large dorsal foramen is a smaller foramen, as also seen in
285 juvenile *C. casuarius* (ROM 759: Evans et al., 2005).

286 In lateral aspect, the preserved portion of the dorsal process extends dorsally, forming an
287 angle of ~151° with the anterodorsal edge of the maxillary body. This angle is similar to that

seen in juvenile *C. casuarius* (e.g., ROM 759) and *L. lambei* (e.g., ROM 758), as well as *V. coahuilensis* (Gates et al., 2007), but differs from the more obtuse angles seen in subadult *H. stebingeri* (TMP 1994.385.0001: Brink et al., 2011), juvenile *H. altispinus* (CMN 2247: Evans, 2010), and juvenile *Parasaurolophus* (RAM 14000: Farke et al., 2013). The lateral aspect of the dorsal process is mostly occupied by the sutural surface for the jugal, which is anteriorly delimited by a distinct, roughly arcuate ridge. The shape of the ridge indicates that the anterior process of the jugal was broadly rounded, as in most lambeosaurines (Lull & Wright, 1942; Evans et al., 2005; Evans, 2010; Brink et al., 2011), rather than distinctly pointed as typically observed in hadrosaurines and *Parasaurolophus* (Horner, 1983, 1992; Prieto-Márquez & Norrell, 2010; Bell, 2011a; Prieto-Márquez, 2012; Xing et al., 2017).

The ectopterygoid ridge projects from the maxilla laterally at a level ventral to the contact surface for the jugal, and extends anteroposteriorly along the posterior two-thirds of the preserved maxillary body. In lateral aspect, the ridge is mostly parallel to the tooth row but is deflected ventrally at the posterior end. In dorsal view and posterior to the dorsal process, the ectopterygoid ridge forms a mediolaterally broad shelf. Viewed posteriorly, the lateral margin of the shelf forms a lip curving ventrally similar to *Parasaurolophus* sp. (RAM 14000: Farke et al., 2013), *M. laticaudus* (Prieto-Márquez et al., 2012) and *H. altispinus* (CMN 8675: Evans, 2010). The ectopterygoid ridge partially covers the posteriormost of a series of three foramina piercing the lateral surface of the maxillary body. Although these foramina consistently occur in the same general area in lambeosaurines, the specific number, shape, and position of these foramina are subject to individual and ontogenetic variation (Evans, 2010).

The nearly horizontal maxillary tooth row extends anteroposteriorly along the entire preserved length of the maxilla. The incomplete tooth row includes 23 identifiable tooth families,

311 which alternate between one or two functional teeth on the occlusal surface. The number of
312 functional teeth per tooth family ranges from one to three in hadrosaurids (Horner et al., 2004).

313 *Postorbital*—The nearly complete left postorbital (UALVP 59902) is triradiate in lateral
314 view, as is typical for hadrosaurids (Lull & Wright, 1942). Three processes are preserved; the
315 anterior process, anteroventrally oriented jugal process, and posteriorly oriented squamosal
316 process (Fig. 7). The postorbital has undergone evident diagenetic distortion, the dorsal and
317 lateral surfaces having been flattened into one plane. In connection with this, there is a large
318 depression on the dorsal surface of the anterior process and a corresponding sinuous crack on the
319 ventral surface. Although such a crack may represent a groove for nerves and/or blood vessels,

320 The anterior process is broad mediolaterally and triangular, with a deeply interdigitated
321 sutural surface for the prefrontal along its anteromedial margin. The prefrontal sutural surface
322 terminates posteriorly at a small medial process, marking the separation between the articular
323 contacts for the prefrontal and the frontal. Accordingly, the frontal was excluded from the orbital
324 margin, as is typical in lambeosaurines (Horner et al., 2004). The medial process is
325 dorsoventrally broad at its base, and tapers medially, suggesting that it underlay the prefrontal
326 and frontal contact and was thus not visible in dorsal view. Posterior to the medial process, the
327 sutural surface for the frontal is less interdigitated than that for the prefrontal and bears a
328 longitudinally oriented groove that opens dorsomedially. In dorsal view, the frontal sutural
329 surface is distinctly concave, owing to the aforementioned medial process combined with a more
330 posteriorly positioned one that would have extended medially to contact the parietal (Horner,
331 1992; Evans et al., 2005; Evans, 2010). The ventral margin of the anterior process of the
332 postorbital and the anterior margin of the jugal process form the posterodorsal rim of the orbit.

The orbital rim is slightly rugose and is not pierced by a foramen as seen in other taxa, although both of these features are subject to intraspecific variation (Horner, 1983, 1992).

The jugal process is damaged at its midpoint, resulting in unnatural anterior deflection of the ventral end. The lateral surface of the jugal process is concave, as seen in the juvenile *C. casuarius* (AMNH 5461), and is broader anteroposteriorly than that of *Parasaurolophus*, though not to the extent seen in *Edmontosaurus* (Parks, 1922; Wiman, 1931; Ostrom, 1961, 1963; Campione & Evans, 2011). The medial surface of the jugal process bears a prominent ridge that bifurcates medially to form a V-shaped fossa for the dorsolateral process of the laterosphenoid. This fossa is typically hemispherical in juvenile hadrosaurines [e.g., *Prosaurolophus maximus* (MOR 447 6.24.6.2), *E. regalis* (ROM 53513 and 53514), and *Brachylophosaurus canadensis* (MOR 1071 6.30.89.4).

The squamosal process is the longest of the main postorbital processes. The squamosal process has a slightly transversely convex dorsal margin, although the convexity is less distinct than in *V. coahuilensis* (Gates et al., 2007). The posterior end of the process is lateromedially expanded, as in other lambeosaurines (Lull & Wright, 1942; Farke et al., 2013), and bifurcated as in all lambeosaurines except *H. altispinus* (Evans, 2010). The ventromedial surface of the squamosal process bears an anteroposteriorly oriented groove, and the area lateral to the groove is broader and more prominent than that medial to the groove.

Histology

A general pattern of bone microstructure is present across the eight sampled humeri. The humeri comprise a thick layer of cortical bone externally and a core of trabecular bone

355 positioned in the centre of the diaphysis. No humeri exhibit a hollow medullary cavity. The
356 trabeculae consist of parallel-fibred bone, although the deepest part of the core of trabecular bone
357 is destroyed in most specimens due to diagenetic modification. External to the inner cancellous
358 bone, most sections show regions of dense Haversian bone that have replaced the primary bone
359 matrix (Fig. 8).

360 The outer half of the cortex comprises woven-fibred bone that ranges from plexiform to
361 reticulate, transitioning to laminar bone towards the periosteal surface. Open osteonal canals are
362 sporadically present on the periosteal surfaces of the humeri, and the lack of external
363 fundamental systems indicates that skeletal growth was incomplete at the time of death.
364 Resorption fronts are present in all sections. However, secondary osteons are rare outside regions
365 of Haversian reconstruction and do not appear within the outer laminar layer. Neither annuli nor
366 lines of arrested growth (LAGs) were observed in any of the sections.

367

368 Taphonomy

369 *Assemblage data*—A total of N=351 vertebrate specimens were collected from the
370 SCBB, including partial and complete teeth, ossified tendons, and bones. The NISP is 273, of
371 which NSPS=142. Almost all (99.7%) of the identifiable specimens are assigned to
372 Hadrosauridae, with only a single tyrannosaurid tooth as direct evidence of a second taxon
373 within the bonebed, although toothmarks suggest other taxa were present before deposition. The
374 three cranial elements described above can be referred to Lambeosaurinae. Based on the number
375 of right humeri that were collected (Fig. 3, Table 1), the current MNI of hadrosaurids is eight.

The maximum preserved lengths of individual specimens range from 10–640 mm (mean = 166 mm; median = 136 mm). Specimen lengths are positively skewed (skewness = 1.4918), the vast majority of elements being <400 mm in total length (Fig. 9). Complete examples of each type of element tend to be uniform in size, suggesting an age-constrained assemblage and supporting the occurrence of a single age class as indicated by the histological results. Complete femora range from 558 mm to 640 mm, placing them in the late juvenile age class of Horner et al. (2000). Total lengths of postcranial elements, scaled against complete *Lambeosaurus* sp. (AMNH 5340) and *Parasaurolophus* sp. (RAM 14000) skeletons (Farke et al., 2013), suggest a total body length estimate of 3.6–4.5 m (Table 4). The absence of LAGs and the presence of multiple microstructural indicators of rapid bone growth observed in the humeral thin-sections further support the juvenile status of the lambeosaurines (see the Histology section for details; Fig. 7).

The vast majority of the bones were found disarticulated, with limited signs of association. The only possible exception pertains to a dentary, a predentary, and a mass of articulated teeth that were all found within an area < 0.5 m^2 (Fig. 2). The representation of Voorhies groups in the SCBB sample is more uniform than would be expected given the structure of the juvenile hadrosaurid skeleton (Table 3; $X^2 = 41.746$, p-value <<0.001). In particular, there is a significant underrepresentation of Voorhies group I relative to groups II and III.

Quarry Data—The lateral extent of the 2018 and 2019 excavations was approximately 18 m, and the total excavation area was 35 m^2 (Fig. 2). A femur recovered ~15 m upstream from the main excavation site, but of similar size and preservation style to those recovered from the quarry, suggests a possible lateral extent of up to 33 m for the SCBB. The fossiliferous horizon is

limited to the bottom 40 cm of a ~2 m thick mudstone layer with no distinct evidence of grading. Crevices (10–15 cm wide) found within the quarry walls suggest widespread slumping and the possible displacement of the entire bonebed from its original position. The density of bones within each grid square ranges from 1 to 30 bones/m^2, with a mean of 7.5 bones/m^2. Preferential alignment of long bones was difficult to determine from the SCBB as Rao's spacing test suggests a significant departure from uniformity (test statistic = 183.6; critical value (at p = 0.05) = 143.8), whilst Kuiper's test of uniformity suggests a uniform distribution (test statistic = 1.05; critical value (at p = 0.05) = 1.7). This inconsistency between tests may be related to the high circular variance ($\sigma^2 = 0.93$) caused by high variability in bone orientation (Fig. 8). Patchiness indices >1 were recorded from both 2018 and 2019 excavations (1.67 and 1.35, respectively) suggesting clumping of specimens rather than a random distribution.

Bone Modification—Of the prepared specimens from the SCBB, 44.2% are complete (Table 4), ranging in size from small cranial elements to relatively large hindlimb elements. A mixture of transverse post-burial fractures and perimortem spiral fractures represents the most common fracture style, observed on 38.9% of the NPSP. Signs of abrasion are rare within the SCBB, with only 13.9% of the NPSP showing low-level abrasion (stages 0 and 1) and <2% exhibiting more severe levels (stages 2 and 3). Similarly, 89.7% of NPSP show little to no signs of weathering (weathering stages 0–1; Table 4, Fig. 4). The remaining 10.3% were observed to be at weathering stage 2.

Biogenic modification of some bones in the sample can be inferred based on the presence of parallel striae, which result from bone–substrate interactions and imply trampling (Behrensmeyer et al., 1986). Approximately 33% of the prepared specimens exhibit such striae. The aforementioned perimortem spiral fractures are also consistent with trampling. Tooth marks

422 are present on 3.8% of NPSP and are represented by pits and conspicuous parallel score marks;
423 these marks primarily occur on limb bones. Given that the tooth marks are predominantly small,
424 U-shaped furrows (Fig. 9), it is likely that they were produced by small scavengers, potentially
425 including small theropods (Bell & Campione, 2014; Bell & Currie, 2015). Some scavenging by
426 larger theropods may have occurred based on the presence of a single shed tyrannosaurid tooth
427 and toothmarks potentially left by smaller tyrannosaurid individuals. Finally, only a single
428 notable pathology was identified, on the supra-acetabular process of an incomplete ilium
429 (UALVP 60540, Fig. 10). The pathology comprises a hemispherical erosion of the lateral surface
430 of the process, with smooth margins but an irregular and rugose internal surface.

431

432 Discussion

433 Systematics of the Spring Creek hadrosaurids

434 The Spring Creek hadrosaurids were preliminarily assigned to the hadrosaurid clade
435 Hadrosaurinae (or Saurolophinae, sensu Prieto-Márquez, 2010) based on the low deltopectoral
436 crests observed on the humeri (Tanke, 2004). The prominence of the crest, however, is known to
437 vary ontogenetically, especially among lambeosaurines (Egi & Weishampel, 2002; Horner et al.,
438 2004), rendering this assignment questionable. The skull elements described in this study
439 represent the first diagnostic cranial material from the SCBB and unequivocally support a
440 lambeosaurine designation based on the following synapomorphies: external naris fully enclosed
441 by the premaxilla, large oblate foramen opening dorsally on the anterodorsal margin of the
442 maxilla, and jugal sutural surface on the maxilla with a broadly rounded anterior margin (Evans,
443 2010; Prieto-Márquez, 2010). Furthermore, the postorbital would have contacted the prefrontal,

444 excluding the frontal from the orbital margin. This condition is typical of lambeosaurines,
445 despite also being present in the hadrosaurines *Prosaurolophus* and *Saurolophus* (Horner, 1992;
446 Horner et al., 2004; Bell, 2011b, 2011a; McGarrity et al., 2013). The other specimens so far
447 recovered from the SCBB are not diagnostic below Hadrosauridae. However, given their
448 consistent size, the absence of conspicuous variations that could indicate the presence of multiple
449 taxa, and the likelihood that the fossils were deposited in a mass mortality event involving a
450 group of juvenile individuals, it is likely that all hadrosaurid specimens from the SCBB pertain to
451 the same species.

452 Unfortunately, the available sample of disarticulated juvenile elements provides only
453 limited diagnostic information, making any taxonomic designation below Lambeosaurinae
454 ambiguous. The relatively acute angle between the body and dorsal process of the maxilla (Fig.
455 3) is more consistent with that seen in *C. casuarius* and *Lambeosaurus* (Lull & Wright, 1942;
456 Evans et al., 2005) than that seen in *Hypacrosaurus* and *Parasaurolophus* (Evans, 2010; Brink et
457 al., 2011; Farke et al., 2013). Similarly, the dorsal convexity of the squamosal process of the
458 postorbital is akin to that in *C. casuarius, L. magnicristatus,* and *Parasaurolophus* (Evans &
459 Reisz, 2007; Farke et al., 2013), though less strongly developed than in *V. coahuilensis* (Gates et
460 al., 2007). By contrast, the more anteriorly attenuated bony naris of the premaxilla (Fig. 4)
461 resembles that of *H. altispinus* and *Lambeosaurus* (Lull & Wright, 1942; Ostrom, 1961; Evans et
462 al., 2005; Gates et al., 2007; Evans, 2010; Brink et al., 2011), and the relatively obtuse snout–
463 crest angle of the premaxilla is most consistent with *H. altispinus* (Evans, 2010; Brink et al.,
464 2014); but note that the squamosal process of the postorbital (UALVP 59902) (Fig. 7) differs
465 from that of *H. altispinus* in being bifurcated (Evans, 2010). Finally, the elongate V-shaped
466 laterosphenoid fossa on the postorbital (Fig. 7) differs from the more typical hemispherical or

short V-shaped fossa seen in other hadrosaurids (Horner, 1992), although this feature may vary across ontogeny.

The SCBB lies within the upper strata of Unit 3 of the Wapiti Formation, which is roughly contemporaneous with the Bearpaw Formation and the Drumheller and Strathmore members of the lower Horseshoe Canyon Formation (Fig. 11). The SCBB lambeosaurines are, therefore, younger than known species of *Corythosaurus*, *Lambeosaurus*, and *Parasaurolophus* from the Dinosaur Park Formation and intermediate in age between *H. stebingeri* and *H. altispinus* from the Two Medicine and Horseshoe Canyon formations, respectively (Horner & Currie, 1994; Brink et al., 2011; Mallon et al., 2012; Eberth & Kamo, 2020). As a result, the SCBB is apparently not contemporaneous with any other hadrosaurid species known from Canada or the U.S.A. (Fig. 11), although it is likely contemporaneous with the Mexican lambeosaurines *V. coahuilensis* (Cerro del Pueblo Formation; Gates et al., 2007) and *M. laticaudatus* (El Gallo Formation; Prieto-Márquez et al., 2012).

The SCBB is geographically located between the northernmost lambeosaurine occurrence, in Alaska (Takasaki et al., 2019), and the lambeosaurines of southern Alberta (Fig. 11). Moreover, the SCBB is at a far higher paleolatitude than the contemporaneous Mexican lambeosaurine localities (Fig. 11). Faunal endemism was suggested for at least Unit 3 of the Wapiti Formation given the presence of *P. lakustai* and *B. certekorum*, both of which are known only from the Pipestone Creek Bonebed (Currie et al., 2008b; Bell & Currie, 2016). Additionally, the occurrence of *E. regalis* in Unit 4 may reflect a shift from endemism to dinosaur cosmopolitanism across Alberta (Bell et al., 2014a).

The fact that the SCBB specimens are either geographically or stratigraphically isolated from all other documented lambeosaurine occurrences, combined with the previously reported

rapid turnover of lambeosaurines from the Dinosaur Park Formation (Mallon et al., 2012) and the conflicting morphological signals described above, suggests that the lambeosaurine material from the SCBB may well represent a new species unique to the Wapiti Formation. However, such a conclusion cannot be considered secure in the absence of more complete, and especially more mature, cranial material that reveals a unique combination of character states. Irrespective of its precise taxonomic identification, the SCBB sample represents the first lambeosaurine material to be reported from the Wapiti Formation. The presence of a lambeosaurine in Unit 3 adds to the evidence that the fauna from this part of the formation, at least, was similar in overall composition to those from the Upper Cretaceous of southern Alberta (Fanti & Catuneanu, 2009; Mallon et al., 2012; Eberth et al., 2013; Fanti et al., 2013; Fowler, 2017; Eberth & Kamo, 2020). Furthermore, this discovery supports the inference that the distribution of lambeosaurines extended into high-latitude regions, recently suggested based on an isolated supraoccipital from the Prince Creek Formation of Alaska (Takasaki et al., 2019).

Taphonomy of the Spring Creek Bonebed

The SCBB is essentially monospecific, containing the remains of at least eight lambeosaurines (thus far represented by 350 hadrosaurid bones) and one tyrannosaurid (represented by a single shed tooth), which are inferred to have been buried in an organic-rich, quiet-water setting based on the bonebeds mud-hosted facies. The tyrannosaurid tooth likely entered the assemblage via scavenging rather than through the same event that caused the death of the lambeosaurines, as non-dental tyrannosaurid material is yet to be recovered from the bonebed. Furthermore, the light to minimal weathering (Table 3; Fig. 3) indicates that all the bones remained exposed for about the same length of time [<12 months; as identified by

513 Behrensmeyer (1978) and Fiorillo (1988)] Together, these observations suggest that the juvenile
514 lambeosaurines perished in a mass mortality event, rather than through gradual attrition
515 (Scherzer & Varricchio, 2010; Bell & Campione, 2014; Chiba et al., 2015; Funston et al., 2016;
516 Ullmann et al., 2017; Campbell et al., 2019).

517 The killing mechanism for the SCBB lambeosaurines remains unknown. The
518 pathological lesion observed on a partial ilium (UALVP 60540; Fig. 10) resembles features
519 resulting from Langerhans Cell Histiocytosis inferred in other hadrosaurids, based on its smooth
520 margin and "wrinkled" internal surface (Rothschild et al., 2020). However, it is intuitively
521 implausible that an osteologically borne disease instigated the mass mortality event. Coastal-
522 plain flooding has been interpreted as the typical source of macrofossil bonebeds throughout the
523 Upper Cretaceous of Alberta (Eberth, 2015). Floodplain deposits, like those hosting the SCBB,
524 are common within Unit 3 of the Wapiti Formation, attesting to periodic inundation while the
525 formation was being deposited (Fanti & Catuneanu, 2009). However, the absence of aquatic
526 vertebrates and the lack of either advanced hydraulic reworking or channel sediments all indicate
527 that the SCBB lambeosaurines did not drown within a channel (Bell & Campione, 2014).
528 Furthermore, in comparison to other ornithischians, hadrosaurids were likely capable of
529 swimming (Henderson, 2014), although such capabilities likely varied ontogenetically.

530 Following the mass mortality event, the lambeosaurine cadavers were exposed long
531 enough for scavenging, trampling, and disarticulation to occur, but were buried before
532 substantial weathering could take place. The ubiquitous disarticulation in the SCBB is most
533 likely as a product of skeletal immaturity, which sees juveniles disarticulating more rapidly than
534 adults (Hill & Behrensmeyer, 1984; Horner & Currie, 1994). Scavenging and trampling may
535 have also contributed to disarticulation, as evident from the observed tooth marks, parallel striae,

536 and spiral fractures. However, scavenging processes were likely minor given the low occurrence
537 of bite-marks (3.8%; Table 4) compared to other sites, such as the Danek Bonebed (30%; Bell &
538 Campione, 2014), Bleriot Ferry Bonebed (~10%; Evans et al., 2015), and Scabby Butte
539 Bonebed: Site 2 (6.2%; Campbell et al., 2019).

540 A significantly higher incidence of bones within Voorhies groups II and III at the SCBB
541 (χ^2=41.746, *P*-value << 0.001; Table 3) indicates the selective removal of some smaller, more
542 transportable elements. Presumably, fluvial factors were the primary sorting mechanism
543 (Voorhies, 1969), although some small elements, including haemal arches and metacarpals, were
544 nonetheless preserved. Tooth marks and parallel striae suggest that scavenging and trampling,
545 respectively, occurred at the SCBB but, given their low incidence, likely represented minor
546 sorting roles compared to fluvial influences. The preservation of hadrosaurid teeth articulated
547 within a dentary (UALVP 59900) is significant because the fragile lingual sheet of bone that
548 keeps the teeth within the dentary is highly susceptible to post-mortem damage, indicating that
549 the SCBB lambeosaurines were buried before such early deterioration could occur (Bell &
550 Campione, 2014). Moreover, the scarcity of teeth within hadrosaurid bonebeds has been used to
551 support a 'bloat-and-float' scenario (Gangloff & Fiorillo, 2010), during which teeth are lost as a
552 result of hydraulic transport, following the loss of the thin lingual sheet. The presence of
553 articulated and isolated teeth in the SCBB in inconsistent this scenario, and suggests little to no
554 transport from the site of death. Although Rao's spacing test suggested a significant NE–SW
555 preferred orientation, the substantial circular variance around this modal orientation (Fig. 9)
556 suggests overall low fluvial influence on long bone alignment. Additionally, high patchiness
557 indices and some skeletal associations suggest little reworking/transport of elements. Overall
558 lack of abrasion in the sample (Table 4) also suggests limited transport (Hunt, 1978; Fiorillo,

559 1988), although the relationship between abrasion and transport can be highly variable
560 (Behrensmeyer, 1982 ; Argast et al., 1987; Eaton et al., 1989). Given the above taphonomic
561 evidence, we cannot unambiguously reject that some transport of elements occurred, and thus the
562 SCBB can be conservatively regarded as a parautochthonous mass mortality bonebed.

563

564 Growth dynamics of the SCBB lambeosaurines

565 Based on their observed bone microstructure the SCBB lambeosaurines were undergoing
566 sustained, but not rapid, growth at their time of death (Horner & Currie, 1994; Horner et al.,
567 2000; Hubner, 2012). The regions of reticular to plexiform bone preserved in the deeper parts of
568 the outer cortex indicate recent periods of rapid growth, whereas the presence of Haversian
569 reconstruction and secondary osteons coupled with the increased organization of the laminar
570 bone towards the periosteal surface suggest that individuals were experiencing a slower growth
571 rate (Horner et al., 1999; Horner et al., 2000; Huttenlocker et al., 2013). No LAGs were observed
572 in any of the sampled humeri. Scaling of limb bones from the SCBB to those of an articulated
573 juvenile *Lambeosaurus* indicates that the individuals had attained a total body length of 3.6–4.5
574 m (Table 2; *Lambeosaurus* data from Farke et al., 2013), which is around half the 7–10 m total
575 body length observed in most adult hadrosaurids or a third of the total ~12 m length reached by
576 giant hadrosaurids (Prieto-Márquez et al., 2012; Hone et al., 2014).

577 Attempts to infer hadrosaurid growth strategies from histological analyses are
578 inescapably convoluted, to say the least. In *Maiasaura peeblesorum*, Horner et al. (2000)
579 identified six distinct ontogenetic stages based on changes in bone microstructure and inferred
580 total lengths of femora: early and late nestling, early and late juvenile, sub-adult, and adult. The

SCBB lambeosaurines bear the greatest histological resemblance to the late juvenile stage, as sectioned humeri display: 1) laminar, plexiform, and reticular bone, 2) Haversian reconstruction, including secondary osteons, 3) spongiose, but not hollow, marrow cavities, and 4) no evidence of LAGs or an external fundamental system (Horner et al., 2000). Late juveniles are hypothesized to exhibit moderate to high growth rates and, based on bone diametral increases, should have reached the late juvenile stage 1.1–2.4 years after hatching (Horner et al., 2000). It is possible, however, that the SCBB lambeosaurines had a different ontogenetic trajectory to that described for *Maiasaura*.

The lack of LAGs among the sampled SCBB humeri is consistent with a late juvenile designation. In *M. peeblesorum*, 0–1 LAGs were indicative of a late juvenile growth stage (Horner et al., 2000). Vanderven et al. (2014) demonstrated that in *E. regalis* LAGs occur more frequently in humeri than in femora of *E. regalis;* a pattern thought to reflect slower humeral growth. A single LAG was observed in the smallest *E. regalis* humerus, although this specimen was ~140 mm longer than the humeri collected from the SCBB. LAGs were previously interpreted as representing annual interruptions in growth (Horner et al., 1999; Horner et al., 2000; Chinsamy et al., 2012; Vanderven et al., 2014; Woodward et al., 2015) and it is, therefore, possible that the lack of LAGs in the SCBB lambeosaurines means that they were not yet a year old at the time of death, despite amassing a considerable size. Alternatively, the lack of LAGs among the sampled SCBB humeri may be the results of environmental, rather than ontogenetic, factors (Chinsamy et al., 2012; Vanderven et al., 2014). The Wapiti Formation represents a geographic transition between polar faunas of Alaska and the more temperate zones of southern Alberta and northern Montana (Bell et al., 2014b). As such, the distinct development of LAGs in *Edmontosaurus* sp. from Alaska could be the result of polar overwintering, with harsher seasons

leading to growth interruption (Chinsamy et al., 2012), although distinct LAGs have also been noted in some hadrosaurids from temperate latitudes (Horner et al., 1999). Nevertheless, the lack of LAGs at the SCBB may suggest that Unit 3 of the Wapiti Formation was deposited under relatively equable climatic conditions (Fanti & Miyashita, 2009).

Alternatively, LAGs may represent cyclical changes in bone apposition caused by hormonal shifts associated with the onset of breeding (Woodward et al., 2015). The tibiae found at the SCBB are ~580 mm, consistent with the size range (560–695 mm) hypothesized for a 3-year-old *M. peeblesorum* (Woodward et al., 2015). However, all *M. peeblesorum* in that size range exhibit LAGs, underscoring the complexity and interspecific diversity of hadrosaurid growth (Horner et al., 1999; Chinsamy et al., 2012; Vanderven et al., 2014; Woodward et al., 2015). If the SCBB lambeosaurine reached sexual maturity at a much larger size than *M. peeblesorum*, this difference might explain the absence of LAGs in sectioned humeri of the former. In any case, the use of LAGs to determine absolute age is evidently ambiguous, given the complications outlined here and elsewhere (Horner et al., 2000; Erickson et al., 2001; Vanderven et al., 2014; Woodward et al., 2015; Slowiak et al., 2020). We, therefore, adopt the more conservative approach of assigning the SCBB lambeosaurines to the late juvenile stage, based on their degree of histological similarity to late juvenile individuals of *M. peeblesorum* (Horner et al., 2000).

Age segregation in hadrosaurids

Taphonomic data and the lack of adult or perinatal material indicate that the SCBB lambeosaurine material is best interpreted as the remains of a group of late juvenile individuals

626 that perished in a single mass mortality event. Accordingly, the composition of the SCBB may
627 reflect a demographic phenomenon known as age segregation—the aggregation and segregation
628 of individuals of the same species based on age, typically in response to resource or spatial
629 limitations (Rogers & Kidwell, 2007; Pelletier et al., 2016). Among dinosaurs, age segregation
630 has been proposed as an explanation for juvenile-dominated bonebed samples of sauropods
631 (Myers & Fiorillo, 2009), theropods (Raath, 1990; Currie, 1998; Zanno & Erickson, 2006;
632 Varricchio et al., 2008), ceratopsians (Gilmore, 1917; Lehman, 2006; Mathews et al., 2007; Zhao
633 et al., 2014), thyreophorans (Galton, 1982; Jerzykiewicz et al., 1993; McWhinney et al., 2004),
634 and ornithopods, including lambeosaurines (Dodson, 1971; Norman, 1987; Forster, 1990;
635 Varricchio & Horner, 1993; Scherzer & Varricchio, 2010; Eberth, 2015; Vila et al., 2016). Food
636 is a limited resource in most ecosystems, and sympatric species often employ interspecific niche
637 partitioning strategies to minimize the adverse effects of competition (Farlow, 1976; du Toit &
638 Cumming, 1999; Lehman, 2001; Mallon & Anderson, 2014). However, ecomorphological data
639 have only distinguished major dinosaurian clades (e.g., ceratopsians vs. hadrosaurids vs.
640 ankylosaurs) and it remains unclear how, and indeed whether, closely related species may have
641 mitigated the effects of mutual competition (Mallon & Anderson, 2014). It is, therefore, possible
642 that in dinosaurs, such as hadrosaurids, such mitigation was achieved via intra- rather than
643 interspecific dynamics, with juveniles and adults partitioning food based on either dietary
644 requirements and/or physiological capabilities. For instance, the fitness costs of dietary
645 synchronization in sauropods (such as those associated with movement to new foraging areas
646 and the need for more resting time) as a result of size difference between juveniles and adults,
647 were possibly eased by age segregation and age-based niche partitioning, a scenario supported by
648 the existence of ontogenetically variable dental microwear patterns (Fiorillo, 1998; Myers &

649 Fiorillo, 2009; Zhao et al., 2014; Pelletier et al., 2016). To date, the possibility of similar
650 ontogenetic variation in dental microwear has not been investigated in hadrosaurids. However,
651 younger hadrosaurids were clearly unable to reach the same maximum feeding heights as adults,
652 implying that juveniles must have had a more restricted feeding envelope unless they were
653 actively fed by mature individuals. Accordingly, the SCBB and other age-segregated bonebeds
654 (Varricchio et al., 2008; Myers & Fiorillo, 2009; Scherzer & Varricchio, 2010; Eberth &
655 Braman, 2012) may be a product of population-level resource partitioning strategies that
656 mitigated competition among diverse communities of megaherbivorous dinosaurs (Mallon et al.,
657 2012; Mallon & Anderson, 2013; Mallon et al., 2013; Mallon & Anderson, 2014).

658 An alternate explanation for age segregation at the SCBB, though one not mutually
659 exclusive with resource partitioning, is that hadrosaurid life history and breeding strategies led to
660 seasonal variation in the age structure among a population (Varricchio, 2011; Zhao et al., 2014).
661 Aggregations of hadrosaurid nesting sites indicate colonial nesting behaviours in both lowland
662 and upland areas (Horner, 1982; Tanke & Brett-Surman, 2001; Fanti & Miyashita, 2009). During
663 nesting times, non-breeding individuals may have segregated away from the breeding
664 population, being relatively large (~50% of typical adult size; Table 2), but potentially still
665 sexually immature (Varricchio et al., 2008; Varricchio, 2011). However, such segregated groups
666 are liable to contain a spectrum of ages (e.g., early–late juveniles; Varricchio et al., 2008; Zhao
667 et al., 2014), which is not the case for the SCBB lambeosaurines. Finally, age segregation could
668 be the result of annually cyclical parental caring behaviours, in which young were reared for an
669 extended period within a yearly cycle, as observed in most modern crocodilian and avian species
670 (Thorbjarnarson & Hernandez, 1993; Davies, 2002). Such parental caring behaviours have been

671 inferred from multiple dinosaur bonebeds, including those of hadrosaurids (Horner & Makela,
672 1979), and supported by egg-adult associations (Varricchio, 2011).

673 It is evident that dinosaurs exhibited complex life histories and behavioural flexibility
674 (e.g. Myers & Fiorillo, 2009; Varricchio, 2011), and there is still much about their palaeoecology
675 that we do not understand (Mallon & Anderson, 2013; Mallon et al., 2013; Mallon & Anderson,
676 2014). Moreover, as we are unable to readily distinguish between males and females in the
677 dinosaur fossil record, and so cannot reject the possibility that age-segregated dinosaur bonebeds
678 were sexually segregated as well (Myers & Fiorillo, 2009; Pelletier et al., 2016), as was implied
679 by Tanke (2004) in his original report on the SCBB as a 'bachelor herd'. Regardless of whether
680 sex-segregation was typical of juvenile hadrosaurid bonebeds, such deposits potentially offer a
681 wealth of insights into growth and social behaviour in these ubiquitous herbivores, and will
682 undoubtedly reward further research.

683

684 Acknowledgements

685 This study was completed as part of BH's Master of Science degree at the University of New
686 England, Australia, supervised by NEC and PRB. Thanks are given to John Scannella and Amy
687 Atwater (Museum of the Rockies), Kevin Seymour (Royal Ontario Museum), Brandon Strilisky
688 and Rebecca Sanchez (Royal Tyrell Museum of Paleontology), and Cam Reed and Calla Scott
689 (Philip J. Currie Dinosaur Museum) for access to and help with their respective collections.
690 Special thanks to Malcolm Lambert (University of New England), for preparing histological
691 samples of TMP specimens. We are grateful to Grande Prairie Regional College for facilitating
692 fieldwork in the Peace Region of northern Alberta, and to the many individuals who volunteered

during the 2018 and 2019 BADP expeditions. This research was funded by a Research Training Program and Rural and Regional Enterprise scholarships to BH, a Dinosaur Research Institute (DRI) Student Project Grant to BH, a DRI Dinosaur Fieldwork in Western Canada to NEC and MJV, and a Natural Sciences and Engineering Research Council Discovery Grant (RGPIN-2017-06246) and an endowment associated with the Philip J. Currie Professorship at the University of Alberta to CS.

References

Argast, S., Farlow, J. O., Gabet, R. M., & Brinkman, D. L. (1987). Transport-induced abrasion of fossil reptilian teeth: implications for the existence of Tertiary dinosaurs in the Hell Creek Formation, Montana. *Geology, 15*(10), 927-930.

Badgley, C. (1986). Taphonomy of Mammalian Fossil Remains from Siwalik Rocks of Pakistan. *Palaeobiology, 12*(2), 119-142.

Behrensmeyer, A. K. (1978). Taphonomic and ecologic information from bone weathering. *Paleobiology, 4*(2), 150-162.

Behrensmeyer, A. K. (1982). Time Resolution in Fluvial Vertebrate Assemblages. *Paleobiology, 8*(3), 211-227.

Behrensmeyer, A. K. (1991). Terrestrial Vertebrate Accumulations. In P. A. Allison & D. E. G. Briggs (Eds.), *Taphonomy: Releasing the Data Locked in the Fossil Record* (Vol. 9, pp. 291-335). New York: Plenum Press.

Behrensmeyer, A. K., Gordon, A. K., & Yanagi, K. D. (1986). Trampling as a cause of bone surface damage and pseudo-cutmarks. *Nature, 319*(6056), 768-771.

715 Bell, P. R. (2011a). Cranial Osteology and Ontogeny of *Saurolophus angustirostris* from the Late
716 Cretaceous of Mongolia with Comments on *Saurolophus osborni* from Canada. *Acta*
717 *Palaeontologica Polonica, 56*(4), 703-722. doi:10.4202/app.2010.0061
718 Bell, P. R. (2011b). Redescription of the skull of *Saurolophus osborni* Brown 1912 (Ornithischia:
719 Hadrosauridae). *Cretaceous Research, 32*(1), 30-44. doi:10.1016/j.cretres.2010.10.002
720 Bell, P. R., & Campione, N. E. (2014). Taphonomy of the Danek Bonebed: a monodominant
721 *Edmontosaurus* (Hadrosauridae) bonebed from the Horseshoe Canyon Formation, Alberta.
722 *Canadian Journal of Earth Sciences, 51*(11). doi:10.1139/cjes-2014-0062
723 Bell, P. R., & Currie, P. J. (2016). A high-latitude dromaeosaurid, *Boreonykus certekorum*, gen. et sp. nov.
724 (Theropoda), from the upper Campanian Wapiti Formation, west-central Alberta. *Journal of*
725 *Vertebrate Paleontology, 36*(1). doi:10.1080/02724634.2015.1034359
726 Bell, P. R., Fanti, F., Currie, P. J., & Arbour, V. M. (2014a). A Mummified Duck-Billed Dinosaur with a Soft-
727 Tissue Cock's Comb. *Current Biology, 24*(1), 70-75. doi:10.1016/j.cub.2013.11.008
728 Bell, P. R., Fanti, F., & Sissons, R. (2013). A possible pterosaur manus track from the Late Cretaceous of
729 Alberta. *Lethaia, 46*, 274-279.
730 Bell, P. R., Sissons, R., Burns, M. E., Fanti, F., & Currie, P. J. (2014b). New Saurolophine Material from the
731 Upper Campanian–lower Maastrichtian Wapiti Formation, West-Central Alberta. In D. Eberth &
732 D. C. Evans (Eds.), *Hadrosaurs* (pp. 174-190). Bloomington, IN: Indiana University Press.
733 Blob, R. W., & Badgley, C. (2007). Numerical Methods for Bonebed Analysis. In R. R. Rogers, D. A. Eberth,
734 & A. R. Fiorillo (Eds.), *Bonebeds: Genesis, Analysis, and Paleobiological Significance* (pp. 333-
735 396). Chicago and London: The University of Chicago Press.
736 Brink, K. S., Zelenitsky, D. K., Evans, D. C., Therrien, F., & Horner, J. R. (2011). A sub-adult skull of
737 *Hypacrosaurus stebingeri* (Ornithischia: Lambeosaurinae): anatomy and comparison. *Historical*
738 *Biology, 23*(1), 63-72. doi:10.1080/08912963.2010.499169

739 Brink, K. S., D. K. Zelenitsky, D. C. Evans, J. R. Horner, and F. Therrien. 2014. Cranial Morphology and
740 Variation in *Hypacrosaurus stebingeri* (Ornithischia: Hadrosauridae). In D. Eberth & D. C. Evans
741 (Eds.), *Hadrosaurs* (pp. 245–265). Bloomington, IN: Indiana University Press.
742 Britt, B. B., Eberth, D. A., Scheetz, R. D., Greenhalgh, B. W., & Stadtman, K. L. (2009). Taphonomy of
743 debris-flow hosted dinosaur bonebeds at Dalton Wells, Utah (Lower Cretaceous, Cedar
744 Mountain Formation, USA). *Palaeogeography, Palaeoclimatology, Palaeoecology, 280*(1-2), 1-
745 22. doi:10.1016/j.palaeo.2009.06.004
746 Campbell, J. A., Ryan, M. J., & Anderson, J. F. (2019). A taphonomic analysis of a multitaxic bonebed
747 from the St. Mary River Formation (uppermost Campanian to lowermost Maastrichtian) of
748 Alberta, dominated by cf. *Edmontosaurus regalis* (Ornithischia: Hadrosauridae), with significant
749 remains of *Pachyrhinosaurus canadensis* (Ornithischia: Ceratopsidae). *Canadian Journal of Earth*
750 *Sciences, 00*, 1-13.
751 Campione, N. E., & Evans, D. C. (2011). Cranial Growth and Variation in Edmontosaurs (Dinosauria:
752 Hadrosauridae): Implications for Latest Cretaceous Megaherbivore Diversity in North America.
753 *PLoS One, 6*(9), e25186. doi:10.1371/journal.pone.0025186
754 Chiba, K., Ryan, M. J., Braman, D. R., Eberth, D. A., Scott, E. E., Brown, C. M., . . . Evans, D. C. (2015).
755 Taphonomy of a Monodominant *Centrosaurus Apertus* (Dinosauria: Ceratopsia) Bonebed from
756 the Upper Oldman Formation of Southeastern Alberta. *Palaios, 30*(9), 655-667.
757 doi:10.2110/palo.2014.084
758 Chinsamy, A., Thomas, D. B., Tumarkin-Deratzian, A. R., & Fiorillo, A. R. (2012). Hadrosaurs Were
759 Perennial Polar Residents. *The Anatomical Record, 295*(4), 610-614. doi:10.1002/ar.22428
760 Christians, J. P. (1992). *Taphonomy and Sedimentology of the Mason Dinosaur Quarry. Hell Creek*
761 *Formation (Upper Cretaceous), South Dakota.* (MSc). University of Wisconsin,
762 Currie, P. J. (1998). Possible evidence of gregarious behavior in tyrannosaurids. *GAIA, 15*, 217-277.

763 Currie, P. J., Langston Jr, W., & Tanke, D. H. (2008a). A new species of *Pachyrhinosaurus* (Dinosauria,
764 Ceratopsidae) from the Upper Cretaceous of Alberta, Canada. A New Horned Dinosaur from an
765 Upper Cretaceous Bone Bed in Alberta. In P. J. Currie, W. Langston Jr, & D. H. Tanke (Eds.), *A*
766 *New Horned Dinosaur from an Upper Cretaceous Bone Bed in Alberta. Ottawa: National*
767 *Research Council of Canada* (pp. 1-108). Ottawa: NRC Research Press.
768 Currie, P. J., Langston, J. W., & Tanke, D. H. (2008b). *A new species of Pachyrhinosaurus (Dinosauria,*
769 *Ceratopsidae) from the Upper Cretaceous of Alberta, Canada*.
770 Davies, S. J. J. F. (2002). *Ratites and Tinamous*. Oxford: Ofxord University Press.
771 Dodson, P. (1971). Sedimentology and taphonomy of the Oldman formation (Campanian), dinosaur
772 provincial park, Alberta (Canada). *Palaeogeography, Palaeoclimatology, Palaeoecology, 10*(1),
773 21-74.
774 du Toit, J. T., & Cumming, D. H. M. (1999). Functional significance of ungulate diversity in African
775 savannas and the ecological implications of the spread of pastoralism. *Biodiversity &*
776 *Conservation, 8*, 1643-1661.
777 Eaton, J. G., Kirkland, J. I., & Doi, K. (1989). Evidence of Reworked Cretaceous Fossils and their Bearing
778 on the Existence of Tertiary Dinosaurs. *Palaios, 4*, 281-286.
779 Eberth, D. A. (2015). Origins of dinosaur bonebeds in the Cretaceous of Alberta, Canada. *Canadian*
780 *Journal of Earth Sciences, 52*, 655-681. doi:10.1139/cjes-2014-0200
781 Eberth, D. A., & Braman, D. R. (2012). A revised stratigraphy and depositional history for the Horseshoe
782 Canyon Formation (Upper Cretaceous), southern Alberta plains. *Canadian Journal of Earth*
783 *Sciences, 49*(9), 1053–1086.
784 Eberth, D. A., & Currie, P. J. (2010). Stratigraphy, sedimentology, and taphonomy of the Albertosaurus
785 bonebed (upper Horseshoe Canyon Formation; Maastrichtian), southern Alberta, Canada.
786 *Canadian Journal of Earth Sciences, 47*(9), 1119-1144. doi:10.1139/E10-045

787 Eberth, D. A., Evans, D. C., Brinkman, D. B., Therrien, F., Tanke, D. H., & Russell, L. S. (2013). Dinosaur
788 biostratigraphy of the Edmonton Group (Upper Cretaceous), Alberta, Canada: evidence for
789 climate influence. *Canadian Journal of Earth Sciences, 50*, 701-726.
790 Eberth, D. A., & Getty, M. A. (2005). Ceratopsian bonebeds: occurence, origins, and significance. In P. J.
791 Currie & E. B. Koppelhus (Eds.), *Dinosaur Provincial Park: A Spectacular Ancient Ecosystem*
792 *Revealed* (pp. 501-536). Bloomington, Indianapolis: Indiana University press.
793 Eberth, D. A., & Kamo, S. L. (2020). High-precision U–Pb CA–ID–TIMS dating and chronostratigraphy of
794 the dinosaur-rich Horseshoe Canyon Formation (Upper Cretaceous, Campanian–Maastrichtian),
795 Red Deer River valley, Alberta, Canada. *Canadian Journal of Earth Sciences, 00*, 1-18.
796 Eberth, D. A., Rogers, R. R., & Fiorillo, A. R. (2007a). A practical approach to the study of bonebeds. In R.
797 R. Rogers, D. A. Eberth, & A. R. Fiorillo (Eds.), *Bonebeds: genesis, analysis, and paleobiological*
798 *significance* (pp. 256-331). Chicago and London: University of Chicago.
799 Eberth, D. A., Shannon, M., & Noland, B. G. (2007b). A Bonebeds Database: Classification, Biases, and
800 Patterns of Occurence. In R. R. Rogers, D. A. Eberth, & A. R. Fiorillo (Eds.), *Bonebeds: Genesis,*
801 *Analysis, and Palaeobiological Significance* (pp. 103-220). Chicago and London: The University of
802 Chicago Press.
803 Egi, N., & Weishampel, D. B. (2002). Morphometric analyses of humeral shapes in hadrosaurids
804 (Ornithopoda, Dinosauria). *Senckenbergiana lethaea, 82*(1), 43-57.
805 Erickson, G. M., Rogers, K. C., & Yerby, S. A. (2001). Dinosaurian growth patterns and rapid avian growth
806 rates. *Nature, 412*, 429-433.
807 Evans, D. C. (2010). Cranial anatomy and systematics of *Hypacrosaurus altispinus*, and a comparative
808 analysis of skull growth in lambeosaurine hadrosaurids (Dinosauria: Ornithischia). *Zoological*
809 *Journal of the Linnean Society, 159*(2), 398-434. doi:10.1111/j.1096-3642.2009.00611.x

Evans, D. C., Eberth, D. A., Ryan, M. l. J., & Therrien, F. (2015). Hadrosaurid (*Edmontosaurus*) bonebeds from the Horseshoe Canyon Formation (Horsethief Member) at Drumheller, Alberta, Canada: geology, preliminary taphonomy, and significance. *Canadian Journal of Earth Sciences, 52*(8), 642-654. doi:10.1139/cjes-2014-0184

Evans, D. C., Forster, C. A., & Reisz, R. R. (2005). The Type Specimen of *Tetragonosaurus erectofrons* (Ornithischia: Hadrosauridae) and the Identification of Juvenile Lambeosaurines. In P. J. Currie & E. B. Koppelhus (Eds.), *Dinosaur Provincial Park: a spectacular ancient ecosystem revealed* (pp. 349-366): Indiana University Press.

Evans, D. C., & Reisz, R. R. (2007). Anatomy and Relationships of *Lambeosaurus magnicristatus*, a crested hadrosaurid dinosaur (Ornithischia) from the Dinosaur Park Formation, Alberta. *Journal of Vertebrate Paleontology, 27*(2), 373-393. doi:10.1671/0272-4634(2007)27[373:Aarolm]2.0.Co;2

Evans, D. C., Reisz, R. R., & Dupuis, K. (2007). A juvenile Parasaurolophus (Ornithischia: Hadrosauridae) braincase from Dinosaur Provincial Park, Alberta, with comments on crest ontogeny in the genus. *Journal of Vertebrate Paleontology, 27*(3), 642-650. doi:10.1671/0272-4634(2007)27[642:Ajpohb]2.0.Co;2

Evans, D. C., Sues, H., Bavington, R., & Campione, N. E. (2009). An unusual hadrosaurid braincase from the Dinosaur Park Formation and the biostratigraphy of Parasaurolophus (Ornithischia: Lambeosaurinae) from southern Alberta. *Canadian Journal of Earth Sciences, 46*(11), 791-800. doi:10.1139/e09-050

Fanti, F., Bell, P. R., & Sissons, R. L. (2013). A diverse, high-latitude ichnofauna from the Late Cretaceous Wapiti Formation, Alberta, Canada. *Cretaceous Research, 41*, 256-269.

Fanti, F., & Catuneanu, O. (2009). Stratigraphy of the Upper Cretaceous Wapiti Formation, west-central Alberta, Canada. *Canadian Journal of Earth Sciences, 46*(4), 263-286. doi:10.1139/e09-020

833 Fanti, F., & Catuneanu, O. (2010). Fluvial sequence stratigraphy: the Wapiti Formation, West-Central
834 Alberta, Canada. *Journal of Sedimentary Research, 80*(4), 320-338. doi:10.2110/jsr.2010.033
835 Fanti, F., Currie, P. J., & Burns, M. E. (2015). Taphonomy, age, and paleoecological implication of a new
836 *Pachyrhinosaurus* (Dinosauria: Ceratopsidae) bonebed from the Upper Cretaceous (Campanian)
837 Wapiti Formation of Alberta, Canada. *Canadian Journal of Earth Sciences, 52*(4), 250-260.
838 doi:10.1139/cjes-2014-0197
839 Fanti, F., & Miyashita, T. (2009). A high latitude vertebrate fossil assemblage from the Late Cretaceous of
840 west-central Alberta, Canada: evidence for dinosaur nesting and vertebrate latitudinal gradient.
841 *Palaeogeography, Palaeoclimatology, Palaeoecology, 275*(1-4), 37-53.
842 doi:10.1016/j.palaeo.2009.02.007
843 Farke, A. A., Chok, D. J., Herrero, A., Scolieri, B., & Werning, S. (2013). Ontogeny in the tube-crested
844 dinosaur *Parasaurolophus* (Hadrosauridae) and heterochrony in hadrosaurids. *PeerJ, 1*, e182.
845 doi:10.7717/peerj.182
846 Farlow, J. O. (1976). A consideration of the trophic dynamics of a Late Cretaceous large dinosaur
847 community (Oldman Formation). *Ecology, 57*, 841-857.
848 Fiorillo, A. R. (1988). Taphonomy of Hazard Homestead Quarry (Ogallala Group), Hitchcook County,
849 Nebraska. *Contributions to Geology, 26*(2), 57-97.
850 Fiorillo, A. R. (1998). Dental microwear patterns of the sauropod dinosaurs *Camarasaurus* and
851 *Diplodocus*: evidence for resource partitioning in the Late Jurassic of North America. *Historical*
852 *Biology, 13*, 1-16.
853 Forster, C. A. (1990). Evidence for juvenile groups in the ornithopod dinosaur *Tenontosaurus tilletti*
854 Ostrom. *Journal of Paleontology, 64*(1), 164-165.

855 Fowler, D. W. (2017). Revised geochronology, correlation, and dinosaur stratigraphic ranges of the
856 Santonian-Maastrichtian (Late Cretaceous) formations of the Western Interior of North America.
857 *PLoS One, 12*(11).
858 Funston, G. F., Currie, P. J., Eberth, D. A., Ryan, M. J., Chinzorig, T., Badamgarav, D., & Longrich, N. R.
859 (2016). The first oviraptorosaur (Dinosauria: Theropoda) bonebed: evidence of gregarious
860 behaviour in a maniraptoran theropod. *Scientific Reports, 6*(35782).
861 Galton, P. M. (1982). Juveniles of the stegosaurian dinosaur *Stegosaurus* from the Upper Jurassic of
862 North America. *Journal of Vertebrate Paleontology, 2*, 47-62.
863 Gangloff, R. A., & Fiorillo, A. R. (2010). Taphonomy and Paleoecology of a Bonebed from the Prince
864 Creek Formation, North Slope, Alaska. *Palaios, 25*(5-6), 299-317. doi:10.2110/palo.2009.p09-
865 103r
866 Gates, T. A., Sampson, S. D., De Jesús, C. R. D., Zanno, L. E., Eberth, D., Hernandez-Rivera, R., . . . Kirkland,
867 J. I. (2007). Velafrons coahuilensis, a new lambeosaurine hadrosaurid (Dinosauria: Ornithopoda)
868 from the late Campanian Cerro del Pueblo Formation, Coahuila, Mexico. *Journal of Vertebrate*
869 *Paleontology, 27*(4), 917-930. doi:10.1671/0272-4634(2007)27[917:Vcanlh]2.0.Co;2
870 Getty, M., Eberth, D. A., Brinkman, D. B., & Ryan, M. (1998). Taphonomy of three *Centrosaurus*
871 bonebeds in the Dinosaur Park Formation, Alberta. *Journal of Vertebrate Paleontology, 18*.
872 Gilmore, C. W. (1917). *Brachyceratops*, a ceratopsian dinosaur from the Two Medicine Formation of
873 Montana with notes on associated reptiles. *United States Geological Survey Professional Paper,*
874 *103*, 1-45.
875 Henderson, D. M. (2014). Duck Soup: The Floating Fates of Hadrosaurs and Ceratopsians at Dinosaur
876 Provincial Park. In D. A. Eberth & D. C. Evans (Eds.), *Hadrosaurs* (pp. 459-466). Bloomington and
877 Indianapolis Indian University Press.

878 Hill, A., & Behrensmeyer, A. K. (1984). Disarticulation patterns in some modern East African mammals.
879 *Palaeobiology, 10*(3), 366-376.
880 Hone, D. W., Sullivan, C., Zhao, Q., Wang, K., & Xu, X. (2014). Body size distribution in a death
881 assemblage of a colossal hadrosaurid from the Upper Cretaceous of Zhucheng, Shandong
882 Province, China. In D. A. Eberth & D. C. Evans (Eds.), *Hadrosaurs* (pp. 524-531). Bloomington:
883 Indiana University Press.
884 Horner, J. R. (1982). Evidence of colonial nesting and 'site fidelity' among ornithschian dinosaurs.
885 *Nature, 297*, 675-676.
886 Horner, J. R. (1983). Cranial Osteology and Morphology of the Type Specimen of *Maiasaura peeblesorum*
887 (Ornithischia: Hadrosauridae), with Discussion of Its Phylogenetic Position. *Journal of Vertebrate*
888 *Paleontology, 3*(1), 29-38.
889 Horner, J. R. (1992). Cranial morphology of *Prosaurolophus* (Ornithischia: Hadrosauridae) with
890 descriptions of two new hadrosaurid species and an evaluation of hadrosaurid phylogenetic
891 relationships. *Museum of the Rockies Occasional Paper, 2*, 1-119.
892 Horner, J. R. (1999). Egg clutches and embryos of two hadrosaurian dinosaurs. *Journal of Vertebrate*
893 *Paleontology, 19*(4), 607-611. doi:10.1080/02724634.1999.10011174
894 Horner, J. R., & Currie, P. J. (1994). Embryonic and neonatal morphology and ontogeny of a new species
895 of *Hypacrosaurus* (Ornithischia, Lambeosauridae) from Montana and Alberta. In K. Carpenter, K.
896 F. Hirsch, & J. R. Horner (Eds.), *Dinosaur Eggs and Babies* (pp. 312-336). Cambridge: University of
897 Cambridge.
898 Horner, J. R., De Ricqles, A., & Padian, K. (2000). Long bone histology of the hadrosaurid dinosaur
899 *Maiasaura peeblesorum* growth dynamics and physiology based on an ontogenetic series of
900 skeletal elements. *Journal of Vertebrate Paleontology, 20*(1), 115-129.

901 Horner, J. R., & Makela, R. (1979). Nest of juveniles provides evidence of family structure among
902 dinosaurs. *Nature, 282*(5736).
903 Horner, J. R., Ricqles, A. D., & Padian, K. (1999). Variation in skeletolochronology indicators: Implications
904 for age assessment and physiology. *Palaeobiology, 25*(3), 295-304.
905 Horner, J. R., Weishampel, D. B., & Forster, C. A. (2004). Hadrosauridae. In D. B. Weishampel, P. Dodson,
906 & H. Osmolska (Eds.), *The Dinosauria, second edition* (pp. 438-463). Berkeley: University of
907 California Press.
908 Hubner, T. R. (2012). Bone Histology in *Dysalotosaurus lettowvorbecki* (Ornithischia: Iguanodontia) –
909 Variation, Growth, and Implications. *PLoS One, 7*(1).
910 Hunt, R. M. (1978). Depositiona setting of a Miocene mammal assemblage, Sioux County, Nebraska
911 (U.S.A.). *Palaeogeography, Palaeoclimatology, Palaeoecology, 24*, 1-52.
912 Huttenlocker, A. K., Woodward, H. N., & Hall, B. K. (2013). *The Biology of Bone*. Berkeley: University of
913 California Press.
914 Jerzykiewicz, T., Currie, P. J., Eberth, D. A., Johnston, P. A., Koster, E. H., & Zheng, J. J. (1993). Djadokhta
915 Formation correlative strata in Chinese Inner Mongolia: an overview of the stratigraphy,
916 sedimentary geology, and paleontology and comparisons with the type locality in the pre-Altai
917 Gobi. *Canadian Journal of Earth Sciences, 30*(10), 2180-2195.
918 Keenan, S. W., & Scannella, J. B. (2014). Paleobiological implications of a *Triceratops* bonebed from the
919 Hell Creek Formation, Garfield County, northeastern Montana. In G. P. Wilson, W. A. Clemens, J.
920 R. Horner, & J. H. Hartman (Eds.), *Through the End of the Cretaceous in the Type Locality of the*
921 *Hell Creek Formation in Montana and Adjacent Areas* (Vol. 503): Geological Society of America.
922 Lehman, T. M. (2001). Late Cretaceous dinosaur provinciality. In D. H. Tanke & K. Carpenter (Eds.),
923 *Mesozoic vertebrate life* (pp. 310-328). Bloomington: Indiana University Press.

924 Lehman, T. M. (2006). Growth and Population Age Structure in the Horned Dinosaur *Chasmosaurus*. In K.
925 Carpenter (Ed.), *Horns and Beaks: Ceratopsian and Ornithopod Dinosaurs* (pp. 259-318).
926 Bloomington and Indianapolis: Indiana University Press.
927 Lucas, S. G., & Sullivan, R. M. (2006). The Kirtlandian land-vertebrate "age"–faunal composition,
928 temporal position and biostratigraphic correlation in the nonmarine Upper Cretaceous of
929 western North America. *New Mexico Museum of Natural History and Science Bulletin, 35*, 7-29.
930 Lucas, S. G., Sullivan, R. M., Lichtig, A. J., Dalman, S. G., & Jasinski, S. E. (2016). Late Cretaceous dinosaur
931 biogeography and endemism in the Western Interior Basin, North America: a critical re-
932 evaluation. *New Mexico Museum of Natural History and Science Bulletin, 71*, 195-213.
933 Lull, R. S., & Wright, N. E. (1942). Hadrosaurian Dinosaurs of North America. *Geological Society of*
934 *America – Special Papers, 40*.
935 Mallon, J. C., & Anderson, J. S. (2013). Skull Ecomorphology of Megaherbivorous Dinosaurs from the
936 Dinosaur Park Formation (Upper Campanian) of Alberta, Canada. *PLoS One, 8*(7).
937 Mallon, J. C., & Anderson, J. S. (2014). Implications of beak morphology for the evolutionary
938 paleoecology of the megaherbivorous dinosaurs from the Dinosaur Park Formation (upper
939 Campanian) of Alberta, Canada. *Palaeogeography Palaeoclimatology Palaeoecology, 394*, 29-41.
940 Mallon, J. C., Evans, D. C., Ryan, M. J., & Anderson, J. S. (2012). Megaherbivorous dinosaur turnover in
941 the Dinosaur Park Formation (upper Campanian) of Alberta, Canada. *Palaeogeography,*
942 *Palaeoclimatology, Palaeoecology, 350*, 124-138.
943 Mallon, J. C., Evans, D. C., Ryan, M. J., & Anderson, J. S. (2013). Feeding height stratification among the
944 herbivorous dinosaurs from the Dinosaur Park Formation (upper Campanian) of Alberta,
945 Canada. *BMC Ecol*.

946 Mathews, J., Henderson, M., & Williams, S. (2007). Taphonomy and sedimentology of the first known
947 Triceratops bonebed, Carter County Montana. *Journal of Vertebrate Paleontology, 27*(3), 114a-
948 114a. Retrieved from <Go to ISI>://WOS:000249535400378
949 McGarrity, C. T., Campione, N. E., & Evans, D. C. (2013). Cranial anatomy and variation inProsaurolophus
950 maximus(Dinosauria: Hadrosauridae). *Zoological Journal of the Linnean Society, 167*(4), 531-568.
951 doi:10.1111/zoj.12009
952 McWhinney, L., Matthias, A., & Carpenter, K. (2004). Corticated pressure erosions, or “pitting,” in
953 osteodermal ankylosaur armor. *Journal of Vertebrate Paleontology, 24*, 92A.
954 Morris, W. J. (1970). Hadrosaurian dinosaur bills: morphology and function. *Los Angeles County Museum*
955 *Contributions in Science, 193*.
956 Myers, T. S., & Fiorillo, A. R. (2009). Evidence for gregarious behavior and age segregation in sauropod
957 dinosaurs. *Palaeogeography, Palaeoclimatology, Palaeoecology, 274*(1-2), 96-104.
958 doi:10.1016/j.palaeo.2009.01.002
959 Norman, D. B. (1987). A mass-accumulation of vertebrates from the Lower Cretaceous of Nehden
960 (Sauerland), West-Germany. *Proveedings of the Royal Society London Series B, 230*, 215-255.
961 Ostrom, J. H. (1961). Cranial Morphology of the Hadrosaurian Dinosaurs of North America. *Bulletin of*
962 *the American Museum of Natural History, 122*, 35-186.
963 Ostrom, J. H. (1963). *Parasaurolophus cyrtocristatus:* A Crested Hadrosaurian Dinosaur from New
964 Mexico. *Chicago Natural History Museum, 14*(8).
965 Parks, W. A. (1922). *Parasaurolophus walkeri*: A New Genus and Species of Crested Trachodont
966 Dinosaur. *University of Toronto Studies, Geological Series, 13*, 1-32.
967 Pelletier, L., Chiaradia, A., Kato, A., & Ropert-Coudert, Y. (2016). Fine-scale spatial age segregation in the
968 limited foraging area of an inshore seabird species, the little penguin. *Oecologia, 176*(2), 399-
969 408.

970 Peterson, J. E., Joseph, E., & Bigalke, C. L. (2013). Hydrodynamic Behaviours of Pachycephalosaurid
971 Domes in Controlled Fluvial Settings: A Case Study in Experimental Dinosaur Taphonomy.
972 *Palaios, 28*, 285-292. doi:10.2110/palo.2013.p13-003r
973 Prieto-Márquez, A. (2010). Global phylogeny of hadrosauridae (Dinosauria: Ornithopoda) using
974 parsimony and Bayesian methods. *Zoological Journal of the Linnean Society, 159*, 435-502.
975 Prieto-Márquez, A. (2012). The skull and appendicular skeleton of *Gryposaurus latidens*, a saurolophine
976 hadrosaurid (Dinosauria: Ornithopoda) from the early Campanian (Cretaceous) of Montana,
977 USA. *Canadian Journal of Earth Sciences, 49*, 510-532.
978 Prieto-Márquez, A., Chiappe, L. M., & Joshi, S. H. (2012). The Lambeosaurine Dinosaur *Magnapaulia*
979 *laticaudus* from the Late Cretaceous of Baja California, Northwestern Mexico. *PLoS One, 7*(6),
980 e38207. doi:10.1371/journal.pone.0038207
981 Prieto-Márquez, A., & Gutarra, S. (2016). The 'duck-billed' dinosaurs of Careless Creek (Upper
982 Cretaceous of Montana, USA), with comments on hadrosaurid ontogeny. *Journal of*
983 *Paleontology, 90*(1), 133-146. Retrieved from https://doi.org/10.1017/jpa.2016.42
984 Prieto-Márquez, A., & Norrell, M. A. (2010). Anatomy and Relationships of *Gilmoreosaurus mongoliensis*
985 (Dinosauria: Hadrosauroidea) from the Late Cretaceous of Central Asia. *American Museum*
986 *Novitates, 3694*.
987 Raath, M. A. (1990). Morphological variation in small theropods and its meaning in systematics:
988 evidence from *Syntarsus rhodesiensis*. In K. Carpenter & P. J. Currie (Eds.), *Dinosaur Systematics:*
989 *Approaches and Perspectives* (pp. 92-105). Cambridge: Cambridge University Press.
990 Rogers, R. R., Eberth, D. A., & Fiorillo, A. R. (2007). *Bonebeds: Genesis, Analysis, and Paleobiological*
991 *Significance* (R. R. Rogers, D. A. Eberth, & A. R. Fiorillo Eds.). Chicago and London: The University
992 of Chicago Press.

993 Rogers, R. R., & Kidwell, M. (2007). A Conceptual Framework for the Genesis and Analysis of Vertebrate
994 Skeletal Concentrations. In R. Rogers, D. Eberth, & A. Fiorillo (Eds.), *Bonebeds: Genesis, analysis,*
995 *and paleobiological significance* (pp. 1-65). Chicago and London: The University of Chicago Press.
996 Rothschild, B. M., Tanke, D., Rühli, F., Pokhojaev, A., & May, H. (2020). Suggested Case of Langerhans
997 Cell Histiocytosis in a Cretaceous dinosaur. *Scientific Reports, 10*(2203), 1-10. Retrieved from
998 https://doi.org/10.1038/s41598-020-59192-z
999 Ryan, M. J., & Evans, D. C. (2005). Ornithischian Dinosaurs. In P. J. Currie & E. B. Koppelhus (Eds.),
1000 *Dinosaur Provincial Park: a spectacular ancient ecosystem revealed* (pp. 312-348). Bloomington:
1001 Inidana University Press.
1002 Sampson, S. D., Loewen, M. A., Farke, A. A., Roberts, E. M., Forster, C. A., Smith, J. A., & Titus, A. L.
1003 (2010). New Horned Dinosaurs from Utah Provide Evidence for Intracontinental Dinosaur
1004 Endemism. *PLoS One, 5*(9), e12292. doi:10.1371/journal.pone.0012292
1005 Scherzer, B. A., & Varricchio, D. J. (2010). Taphonomy of a Juvenile Lambeosaurine Bonebed from the
1006 Two Medicine Formation (Campanian) of Montana, United States. *Palaios, 25*(11-12), 780-795.
1007 doi:10.2110/palo.2009.p09-143r
1008 Slowiak, J., Szczygielski, T., Ginter, M., & Fostowicz-Frelik, Ł. (2020). Uninterrupted Growth in a Non-
1009 Polar Hadrosaur Explains the Gigantism Among Duck-Billed Dinosaurs. *Palaeontology*, 1-21.
1010 doi:10.1111/pala.12473
1011 Takasaki, R., Fiorillo, A. R., Kobayashi, Y., Tykoski, R. S., & McCarthy, P. J. (2019). The First Defnite
1012 Lambeosaurine Bone From the Liscomb Bonebed of the Upper Cretaceous Prince Creek
1013 Formation, Alaska, United States. *Scientific Reports, 9*(5384). Retrieved from
1014 https://doi.org/10.1038/s41598-019-41325-8

1015 Tanke, D., & Brett-Surman, M. K. (2001). Evidence of hatchling and nesting-size hadrosaurs (Reptilia:
1016 Ornithischia) from Dinosaur Provincial park (Dinosaur Park Formation: Campanian), Alberta.
1017 *Mesozoic vertebrate life*.
1018 Tanke, D. H. (2004). Mosquitoes and Mud: The 2003 Royal Tyrrell Museum Expedition to the Grande
1019 Prairie Region (northwestern Alberta, Canada). *Alberta Palaeontological Society Bulletin, 19*(2),
1020 3-31.
1021 Thorbjarnarson, J. B., & Hernandez, G. (1993). Reproductive ecology of the Orinoco crocodile
1022 (Crocodylus intermedius) in Venezuela. *Journal of herpetology*, 363-370.
1023 Ullmann, P. V., Shaw, A., Nellermoe, R., & Lacovara, K. J. (2017). Taphonomy of the Standing Rock
1024 Hadrosaur Site, Corson County, South Dakota. *Palaios, 32*(12), 779-796.
1025 doi:10.2110/palo.2017.060
1026 Vanderven, E., Burns, M. E., & Currie, P. J. (2014). Histologic growth dynamic study of *Edmontosaurus*
1027 *regalis* (Dinosauria: Hadrosauridae) from a bonebed assemblage of the Upper Cretaceous
1028 Horseshoe Canyon Formation, Edmonton, Alberta, Canada. *Canadian Journal of Earth Sciences,*
1029 *51*(11), 1023-1033. doi:10.1139/cjes-2014-0064
1030 Varricchio, D. J. (1995). Taphonomy of Jacks-Birthday Site, a Diverse Dinosaur Bonebed from the Upper
1031 Cretaceous Two-Medicine Formation of Montana. *Palaeogeography Palaeoclimatology*
1032 *Palaeoecology, 114*(2-4), 297-323. doi:Doi 10.1016/0031-0182(94)00084-L
1033 Varricchio, D. J. (2011). A distinct dinosaur life history? *Historical Biology, 23*(1), 91-107.
1034 doi:10.1080/08912963.2010.500379
1035 Varricchio, D. J., & Horner, J. R. (1993). Hadrosaurid and lambeosaurid bone beds from the Upper
1036 Cretaceous Two Medicine Formation of Montana: taphonomic and biologic implications.
1037 *Canadian Journal of Earth Sciences, 30*(5), 997-1006.

1038 Varricchio, D. J., Sereno, P. C., Xijin, Z., Lin, T., Wilson, J. A., & Lyon, G. H. (2008). Mud-Trapped Herd
1039 Captures Evidence of Distinctive Dinosaur Sociality. *Acta Palaeontologica Polonica, 53*(4), 567-
1040 578. doi:10.4202/app.2008.0402
1041 Vila, B., Sellés, A. G., & Brusatte, S. L. (2016). Diversity and faunal changes in the latest Cretaceous
1042 dinosaur communities of southwestern Europe. *Cretaceous Research, 57*, 552-564.
1043 Voorhies, M. (1969). *Taphonomy and Population Dynamics of an Early Pliocene Vertebrate Fauna, Knox*
1044 *County, Nebraska*. Laramie: University of Wyoming.
1045 Wiman, C. (1931). *Parasaurolophus tubicens* n. sp. aus der kreide in New Mexico. *Nova Acta Regiae*
1046 *Societatis Scietiarum Upsaliensis Ser IV, 7*, 11.
1047 Woodward, H. N., Freedman Fowler, E. A., Farlow, J. O., & Horner, J. R. (2015). *Maiasaura*, a model
1048 organism for extinct vertebrate population biology: a large sample statistical assessment of
1049 growth dynamics and survivorship. *Paleobiology, 41*(4), 503-527.
1050 Xing, H., Mallon, J. C., & Currie, M. L. (2017). Supplementary cranial description of the types of
1051 *Edmontosaurus regalis* (Ornithischia: Hadrosauridae), with comments on the phylogenetics and
1052 biogeography of Hadrosaurinae. *PLoS One, 12*(4), e0175253. Retrieved from https://doi.org/
1053 10.1371/journal.pone.0175253
1054 Zanno, L., & Erickson, G. (2006). Ontogeny and life history of *Falcarius utahensis*, a primitive
1055 therizinosauroid from the Early Cretaceous of Utah. *Journal of Vertebrate Paleontology, 26*(3),
1056 143A.
1057 Zhao, Q., Benton, M. J., Xu, X., & Sander, P. M. (2014). Juvenile-only clusters and behaviour of the Early
1058 Cretaceous dinosaur *Psittacosaurus*. *Acta Palaeontologica Polonica, 59*(4), 827-834.

1059

1060 **Tables**

Table 1. List of humeri recovered from the Spring Creek Bonebed as seen in Figure 4.

Table 2. Postcranial elements from the Spring Creek lambeosaurine scaled against elements from a complete *Lambeosaurus* sp. (AMNH 5340; from Farke et al., 2013) to estimate total body length.

Table 3. Inventory and categorization of bones in a complete juvenile hadrosaurid skeleton and expected vs observed proportions of Voorhies groups from the Spring Creek Bonebed. Observed proportions were calculated from the number of identifiable specimens (adapted from Varricchio, 1995; Horner et al., 2004; Scherzer & Varricchio, 2010; Bell & Campione, 2014).

Table 4. Taphonomic observations from the Spring Creek Bonebed, including the results of Chi-squared tests on the number of prepared specimens.

Figure Captions

Figure 1. Locality map of main macrofossil localities from the Grande Prairie area and the geographic extent of the Wapiti Formation. (A) Locality map of the main macrofossil localities proximate to Grande Prairie, Alberta, Canada. Numbers indicate the following localities: 1) George Robinson Bonebed (Tanke, 2004); 2) Mummified *Edmontosaurus regalis* skeleton (Bell et al., 2014a); 3) Red Willow hadrosaur (Bell et al., 2014b); 4) Wapiti River *Pachyrhinosaurus* Bonebed (Fanti et al., 2015); 5) Pipestone Creek *Pachyrhinosaurus lakustai* Bonebed (Currie et al., 2008b); 6) Spring Creek Bonebed (red star; this study). (B) Map

1081 illustrating the lateral extent of the Wapiti Formation (in grey) across Alberta and into eastern
1082 British Columbia.

1083 **Figure 2. Quarry map of the Spring Creek Bonebed.** (A) Map of the 2018 and 2019
1084 excavations of the Spring Creek Bonebed by the Boreal Alberta Dinosaur Project (grey: isolated
1085 specimens; white: specimens in concretions). (B) Associated dentary (UALVP 59898), partial
1086 dental battery (UALVP 59887), and predentary (UALVP 59888) from Spring Creek Bonebed.
1087 Reconstruction based on *Hypacrosaurus stebingeri* (Brink et al., 2011). The 10 cm scale bar
1088 applies to the bones in B and the skull reconstruction. (C) Quarry photo of bones in situ.

1089 **Figure 3. Exposures at the Spring Creek Bonebed.** (A) Photograph of the bank exposure at the
1090 Spring Creek Bonebed (indicated by white arrows). (B) Stratigraphic column from the Spring
1091 Creek Bonebed (sediment grains sizes: c, clay; m, mud; fs, fine sand; s, sand). Derek Larson
1092 (175 cm) for scale.

1093 **Figure 4. Right (top) and left (bottom) humeri recovered from the Spring Creek Bonebed**
1094 **and denoting the minimum number of individuals (MNI=eight) and their consistent size.**
1095 Humeri show the typical lack of weathering and abrasion observed throughout the Spring Creek
1096 Bonebed. Additionally, humeri exhibit a variety of fracture styles and diagenetic distortion,
1097 causing the visible morphological variances.

1098 **Figure 5. Left lambeosaurine premaxilla (UALVP 60537) from the Spring Creek Bonebed.**
1099 (A) Lateral view, including life reconstruction based on *Hypacrosaurus stebingeri* (Brink et al.,
1100 2011). Grey region indicates the portion of the premaxilla that was preserved. (B) Dorsal view
1101 with a dashed white line indicating the perimeter of the exposed bony naris. Abbreviations: bn,
1102 bony naris; cdp, caudodorsal process; nv, nasal vestibule; om, oral margin.

Figure 6. Right lambeosaurine maxilla (UALVP 59881b) from the Spring Creek Bonebed. (A) Lateral view, showing hypothetical reconstruction based on *Hypacrosaurus* sp. (MOR 553s). The dashed white line indicates the anterior margin of the sutural surface for the jugal. Black arrows indicate the location of lateral foramina. (B) Medial view. (C) Anterodorsal view. (D) Dorsal view. (E) Ventral view. Abbreviations: af, alveolar foramina; df, dorsal foramen; dp, dorsal process; ec, ectopterygoid ridge; mt, maxillary teeth; ps, premaxillary shelf; sdf, secondary dorsal foramen; ssj, sutural surface for the jugal.

Figure 7. Left lambeosaurine postorbital (UALVP 59902) from the Spring Creek Bonebed. (A) Dorsolateral view. (B) Ventromedial view. White dashed line outlines the shape of the latersphenoid fossa. Note the longitudinal fracture on the medial surface in (B), which could also represent a neurovascular canal. Abbreviations: jp, jugal process; or, orbital rim; sp, squamosal process; ssf, sutural surface for frontal; ssp, sutural surface for parietal; sspf, sutural surface for prefrontal.

Figure 8. Thin sections of Spring Creek Bonebed humeri showing bone microstructure. (A) Thin section of a humerus (UALVP 60539) showing the typical bone microstructure of humeri from the Spring Creek Bonebed, as described in the text. Scale bar = 1 mm. White arrows: 1, cancellous bone; 2, reticular bone; 3, plexiform bone; 4, laminar bone; 5, Haversian bone. (B) Laminar bone from UALVP 60533. Scale bar = 500 μm. (C) Reticular bone from UALVP 60535. Scale bar = 500 μm. (D) Plexiform bone from UALVP 60535. Scale bar = 500 μm. (E) Haversian reconstruction from UALVP 60539. Scale bar = 500 μm.

Figure 9. Distribution of bones at the Spring Creek Bonebed. (A) The positively skewed size distribution of specimens from the bonebed. (B) A rose diagram of the recorded orientations of

long bones from the Spring Creek Bonebed showing a preferential NE–SW modality, but overall high circular variance.

Figure 10. Examples of bone modification from the Spring Creek Bonebed. (A) Unhealed parallel toothmarks (white arrows) on the lateral surface of the left dentary (UALVP 59907) interpreted as post mortem scavenging. (B) Pathology (margin indicated by white arrows) on the lateral surface of the supra-acetabular process (sa) from an incomplete ilium (UALVP 60540).

Figure 11. Biostratigraphy and palaeobiogeography of temporally and spatially proximate Lambeosaurinae from Alberta, Canada, Montana, USA, and Mexico. (A) Biostratigraphic distribution of Lambeosaurinae across strata from Montana, USA (Horner & Currie, 1994; Campbell et al., 2019), western and northeastern Mexico (Lucas & Sullivan, 2006; Gates et al., 2007; Prieto-Márquez et al., 2012; Fowler, 2017), and northwestern Alberta (Fanti & Catuneanu, 2009; this study), and southern Alberta, Canada (Mallon et al., 2012; Eberth et al., 2013; Eberth & Kamo, 2020). The Wapiti and Horseshoe Canyon formations are subdivided into units and members, respectively. Grey stratum represents the marine Bearpaw Formation (BPFm). The dashed range for the Spring Creek lambeosaurines represents a temporal range within Unit 3, between the Pipestone Creek Bonebed (73.5 Ma; (Currie et al., 2008b) and the basal most Horseshoe Canyon Formation (74.4 Ma; (Eberth & Braman, 2012). (B) Palaeobiogeographical distribution of Lambeosaurinae across Montana, USA, Alberta, Canada, and Mexico (Lull & Wright, 1942; Horner & Currie, 1994; Evans & Reisz, 2007; Evans et al., 2007; Gates et al., 2007; Evans et al., 2009; Evans, 2010; Prieto-Márquez et al., 2012). The silhouette of the Spring Creek lambeosaurine and *Magnapaulia laticaudus* were created by Scott Hartman and Dmitry Bogdanov, respectively. Both were vectorized by T. Michael Keesey and used under the creative

1147 commons attribution 3.0 unported license (https://creativecommons.org/licenses/by/3.0/). The
1148 remaining silhouettes were used and modified under the public domain dedication 1.0 license.

1149

1150

Table 1(on next page)

List of humeri recovered from the Spring Creek Bonebed as seen in Figure 4.

Table 1. List of humeri recovered from the Spring Creek Bonebed as seen in Figure 4.

Figure Identifier	Specimen Number	Element	Length (mm)	Used for Histology
A	TMP 1991.137.0005	Right humerus (proximal)	282*	
B	UALVP 60537	Right humerus	261	
C	UALVP 60539	Right humerus	247	✓
D	UALVP 60534	Right humerus	246**	✓
E	UALVP 60536	Right humerus	262**	✓
F	UALVP 60532	Right humerus (distal)	268*	✓
G	UALVP 60535	Right humerus (proximal)	252*	✓
H	UALVP 60541	Right humerus (proximal)	270*	
I	TMP 1991.127.0001	Left humerus	253	
J	UALVP 60533	Left humerus (distal)	231*	✓
K	TMP 1991.137.0009	Left humerus (distal)	279*	✓
L	TMP 1988.94.0002	Left humerus (distal)	235*	
M	TMP 1988.94.0006	Left humerus (distal)	254*	✓
	Humerus length:	Mean = 257mm	sd = 15.5mm	

*Estimated lengths

**Have undergone diagenetic modification

Table 2(on next page)

Postcranial elements from the Spring Creek lambeosaurine scaled against elements from a complete *Lambeosaurus* sp. (AMNH 5340; from Farke et al., 2013) to estimate total body length.

Table 2. Postcranial elements from the Spring Creek lambeosaurine scaled against elements from a complete *Lambeosaurus* sp. (AMNH 5340; from Farke et al., 2013) to estimate total body length.

Taxon	*Lambeosaurus* sp. (Farke et al., 2013)	Lambeosaurinea indet. (this study)
Specimen	AMNH 5340	Spring Creek specimens
Humerus length (mm)	305	257 (0.84)
Femur length (mm)	590	565 (0.96)
Tibia length (mm)	550	580 (1.05)
Fibula length (mm)	530	455 (0.86)
Total Length	4.31m	3.62 – 4.52m*

Brackets indicate scale factor from AMNH 5340

*Estimated body lengths

Table 3(on next page)

Inventory and categorization of bones in a complete juvenile hadrosaurid skeleton and expected vs observed proportions of Voorhies groups from the Spring Creek Bonebed.

Observed proportions were calculated from the number of identifiable specimens (adapted from Varricchio, 1995; Horner et al., 2004; Scherzer & Varricchio, 2010; Bell & Campione, 2014).

Table 3. Inventory and categorization of bones in a complete juvenile hadrosaurid skeleton (adapted from Varricchio, 1995; Horner et al., 2004; Scherzer & Varricchio, 2010; Bell & Campione, 2014), and expected vs observed proportions of Voorhies groups from the Spring Creek Bonebed. Observed proportions were calculated from the number of identifiable specimens.

Voorhies Group I			Voorhies Group II			Voorhies Group III		
Category	**Element**	**Count**	**Category**	**Element**	**Count**	**Category**	**Element**	**Count**
Light cranial elements	Premaxillae	2	Pectoral elements	Sternal plates	2	Limb bones	Humeri	2
	Nasals	2		Coracoids	2		Radii	2
	Lacrimals	2		Scapulae	2		Ulnae	2
	Jugals	2	Dense cranial elements	Maxillae	2		Femora	2
	Quadratojugals	2		Dentaries	2		Tibiae	2
	Postorbitals	2		Braincase	1		Fibulae	2
	Surangulars	2	Tarsals and metapodials	Astragali	2			
	Exoccipitals	2		Metatarsals	6			
	Hyoids	2		Metacarpals	6			
	Squamosals	2						
	Quadrates	2						
	Frontals	2						
	Ectopterygoids	2						
Digital elements	Pedal phalanges	24						
	Manual phalanges	24						
Ribs	Dorsal ribs	36						
Vertebrae (including isolated centra)	Cervical	13						
	Dorsal	18						
	Caudal	50						
	Sacral	9						
Vertebral processes	Transverse processes	84						
	Neural spines	49						
	Haemal arches	35						
	Expected proportion	89.6%		Expected proportion	7.5%		Expected proportion	2.9%
	Observed proportion	48%		Observed proportion	23.3%		Observed proportion	28.7%
Chi-squared results:	X-squared = 41.746							
	df = 2							
	p-value << 0.001							

Table 4(on next page)

Taphonomic observations from the Spring Creek Bonebed, including the results of Chi-squared tests on the number of prepared specimens.

Table 4. Taphonomic observations from the Spring Creek Bonebed, including the results of Chi-squared tests on the number of prepared specimens.

Weathering Stage (Behrensmeyer, 1978; Fiorillo, 1988)	**Observed proportion**	**Abrasion Stage** (Fiorillo, 1988)	**Observed proportion**	**Fracture Style**	**Observed proportion**
Stage 0: No signs of cracking or flaking on bone. Possible years exposed after death: 0-1	72.9%	**Stage 0:** Bone is unabraded, preserving all processes and edges.	84.3%	**Complete:** Bone is preserved in its entirety.	44.2%
Stage 1: Bone is beginning to show signs of longitudinal cracking. Possible years exposed after death: 0-3	16.8%	**Stage 1:** Slight abrasion with some rounding of edges.	13.9%	**Spiral:** Fractures with irregular fracture surfaces preserved from pre-burial.	7.6%
Stage 2: Thin layers of bone flaking, typically associated with longitudinal cracks. Possible years exposed after death: 2-6	10.3%	**Stage 2:** Moderate abrasion in which edges are well-rounded, and processes may or may not be identifiable.	0.9%	**Transverse:** Straight, transverse fractures preserved from post burial.	9.3%
Stage 3: Patches of exposed fibrous texture where concentrically layered bone has been removed. Possible years exposed after death: 4-15+	0%	**Stage 3:** High level of abrasion, edges extremely rounded, original bone shape is barely recognisable.	0.9%	**Mixed:** Both transverse and spiral fractures preserved.	38.9%
Chi-squared results: $X^2 = 71.08$ p-value <<0.001		Chi-squared results: $X^2 = 191.77$ p-value <<0.001		Chi-squared results: $X^2 = 44.538$ p-value <<0.001	
Proportion of specimens observed with toothmarks: 3.8%				Proportion of specimens observed with parallel striae: 28.2%	

Figure 1

Locality map of main macrofossil localities from the Grande Prairie area and the geographic extent of the Wapiti Formation.

(A) Locality map of the main macrofossil localities proximate to Grande Prairie, Alberta, Canada. Numbers indicate the following localities: 1) George Robinson Bonebed (Tanke, 2004); 2) Mummified *Edmontosaurus regalis* skeleton (Bell et al., 2014a); 3) Red Willow hadrosaur (Bell et al., 2014b); 4) Wapiti River *Pachyrhinosaurus* Bonebed (Fanti et al., 2015); 5) Pipestone Creek *Pachyrhinosaurus lakustai* Bonebed (Currie et al., 2008b); 6) Spring Creek Bonebed (red star; this study). (B) Map illustrating the lateral extent of the Wapiti Formation (in grey) across Alberta and into eastern British Columbia.

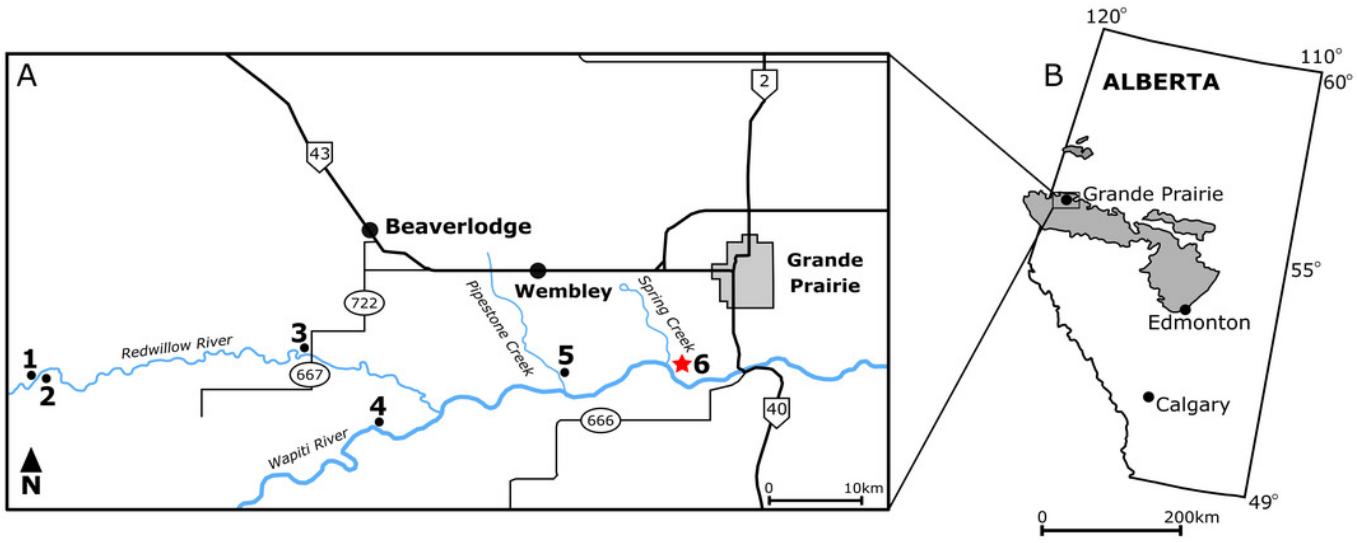

Figure 2

Quarry map of the Spring Creek Bonebed.

(A) Map of the 2018 and 2019 excavations of the Spring Creek Bonebed by the Boreal Alberta Dinosaur Project (grey: isolated specimens; white: specimens in concretions). (B) Associated dentary (UALVP 59898), partial dental battery (UALVP 59887), and predentary (UALVP 59888) from Spring Creek Bonebed. Reconstruction based on *Hypacrosaurus stebingeri* (Brink et al., 2011). The 10 cm scale bar applies to the bones in B and the skull reconstruction. (C) Quarry photo of bones in situ.

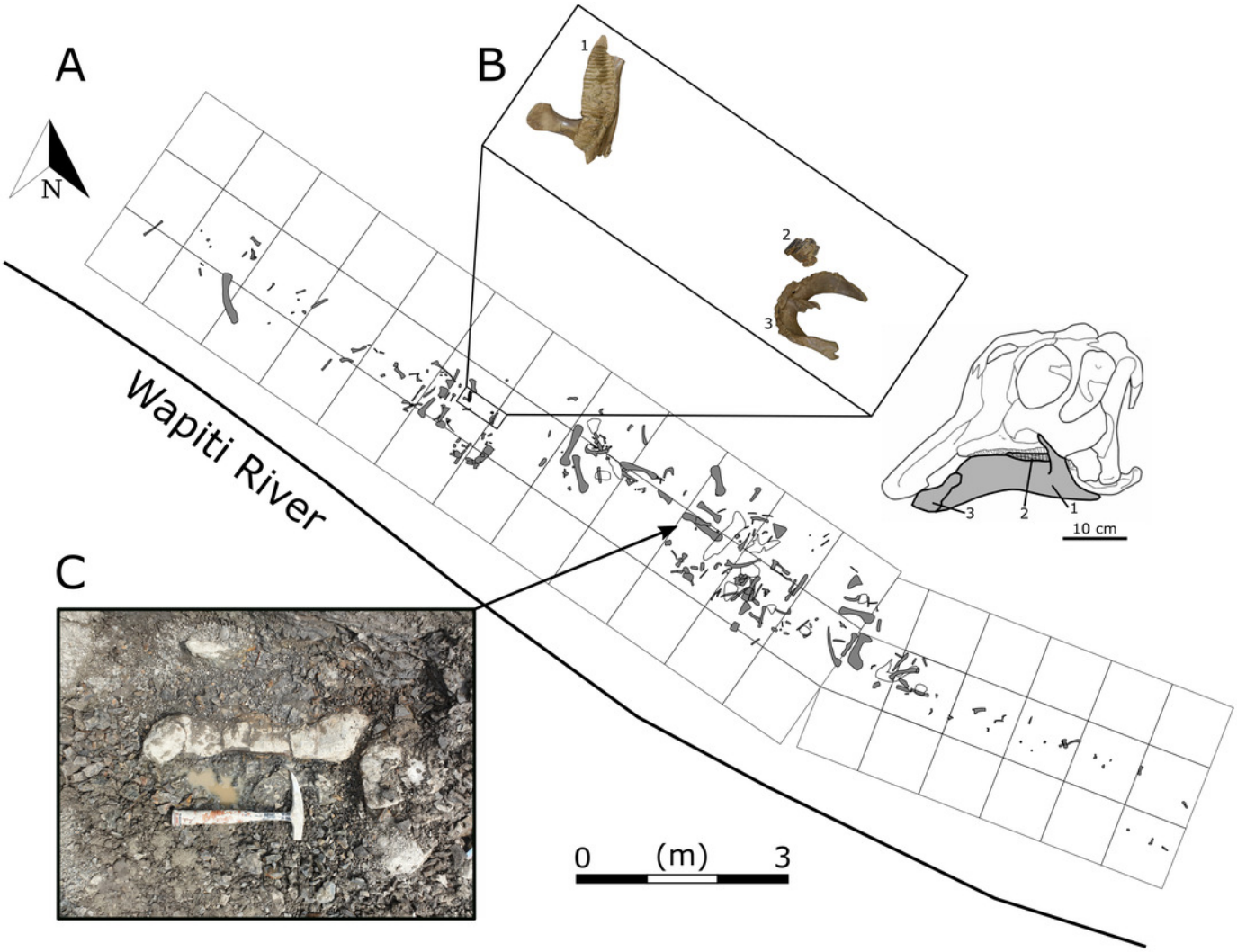

Figure 3

Exposures at the Spring Creek Bonebed.

(A) Photograph of the bank exposure at the Spring Creek Bonebed (indicated by white arrows). (B) Stratigraphic column from the Spring Creek Bonebed (sediment grains sizes: c, clay; m, mud; fs, fine sand; s, sand). Derek Larson (175 cm) for scale.

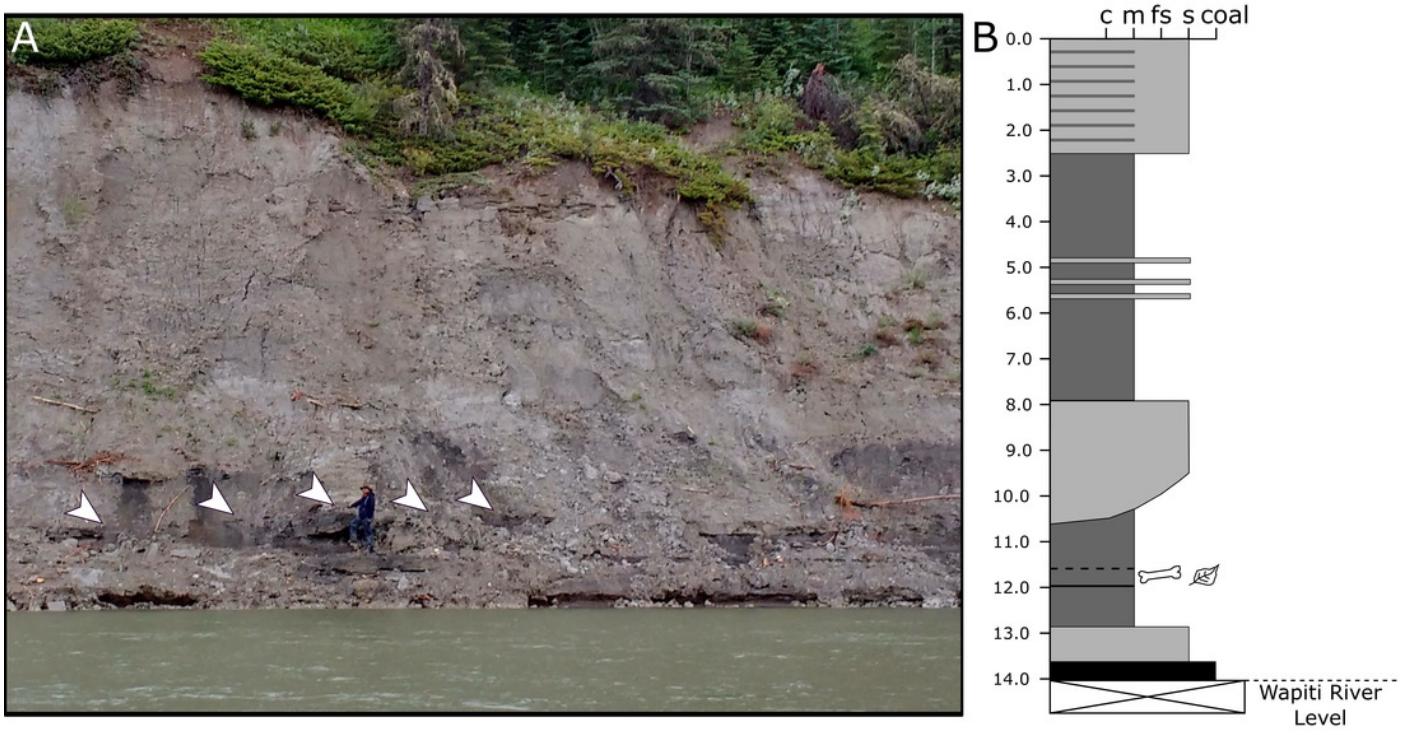

Figure 4

Right (top) and left (bottom) humeri recovered from the Spring Creek Bonebed and denoting the minimum number of individuals (MNI=eight) and their consistent size.

Humeri show the typical lack of weathering and abrasion observed throughout the Spring Creek Bonebed. Additionally, humeri exhibit a variety of fracture styles and diagenetic distortion, causing the visible morphological variances.

Figure 5

Left lambeosaurine premaxilla (UALVP 60537) from the Spring Creek Bonebed.

(A) Lateral view, including life reconstruction based on *Hypacrosaurus stebingeri* (Brink et al., 2011). Grey region indicates the portion of the premaxilla that was preserved. (B) Dorsal view with a dashed white line indicating the perimeter of the exposed bony naris. Abbreviations: bn, bony naris; cdp, caudodorsal process; nv, nasal vestibule; om, oral margin.

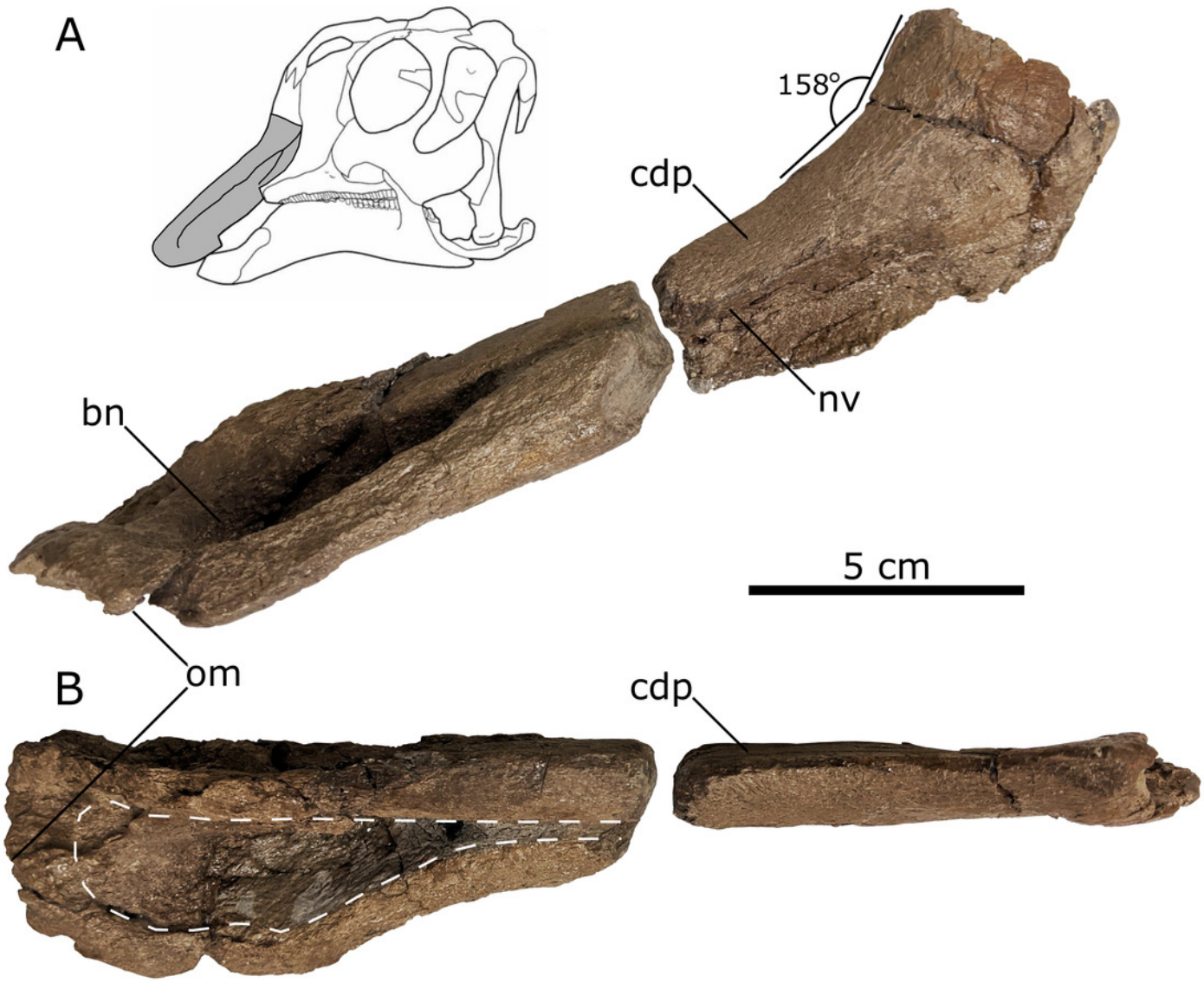

Figure 6

Right lambeosaurine maxilla (UALVP 59881b) from the Spring Creek Bonebed.

(A) Lateral view, showing hypothetical reconstruction based on *Hypacrosaurus* sp. (MOR 553s). The dashed white line indicates the anterior margin of the sutural surface for the jugal. Black arrows indicate the location of lateral foramina. (B) Medial view. (C) Anterodorsal view. (D) Dorsal view. (E) Ventral view. Abbreviations: af, alveolar foramina; df, dorsal foramen; dp, dorsal process; ec, ectopterygoid ridge; mt, maxillary teeth; ps, premaxillary shelf; sdf, secondary dorsal foramen; ssj, sutural surface for the jugal.

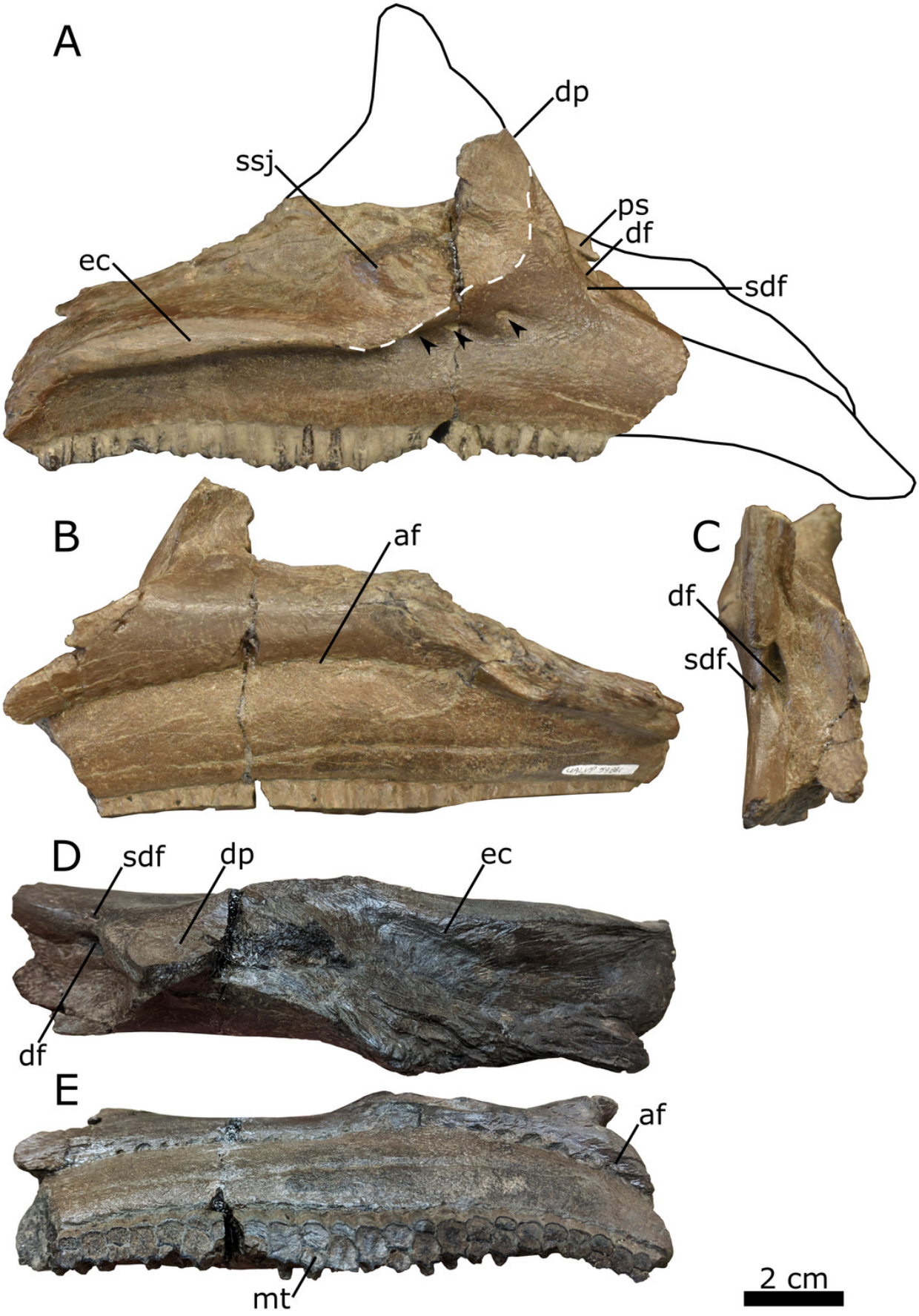
A
dp
ssj
ps
df
ec
sdf
B
af
C
df
sdf
D
sdf
dp
ec
df
E
af
mt
2 cm

Figure 7

Left lambeosaurine postorbital (UALVP 59902) from the Spring Creek Bonebed.

(A) Dorsolateral view. (B) Ventromedial view. White dashed line outlines the shape of the latersphenoid fossa. Note the longitudinal fracture on the medial surface in (B), which could also represent a neurovascular canal. Abbreviations: jp, jugal process; or, orbital rim; sp, squamosal process; ssf, sutural surface for frontal; ssp, sutural surface for parietal; sspf, sutural surface for prefrontal.

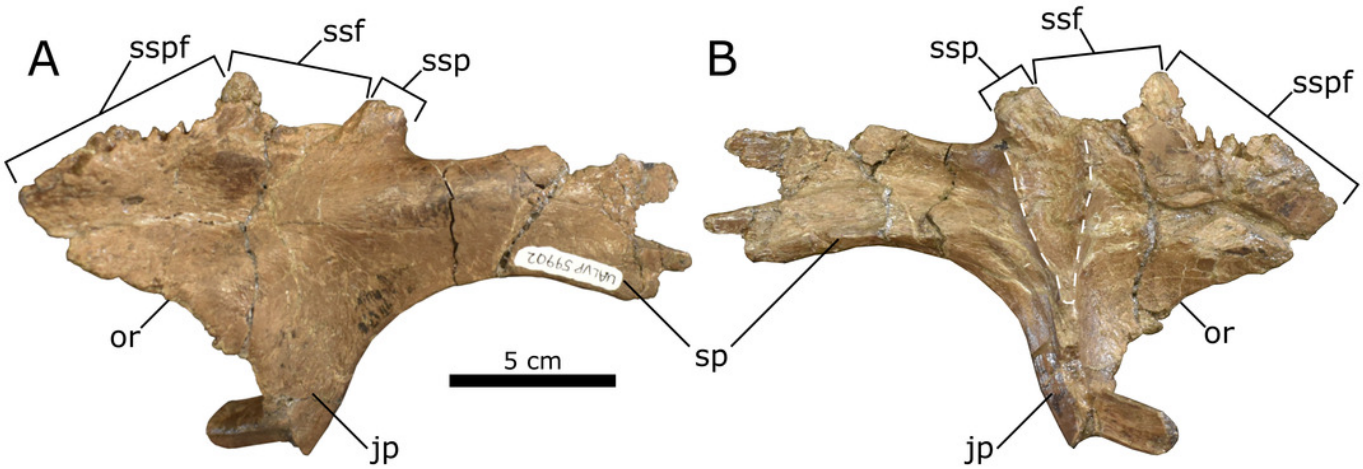

Figure 8

Thin sections of Spring Creek Bonebed humeri showing bone microstructure.

(A) Thin section of a humerus (UALVP 60539) showing the typical bone microstructure of humeri from the Spring Creek Bonebed, as described in the text. Scale bar = 1 mm. White arrows: 1, cancellous bone; 2, reticular bone; 3, plexiform bone; 4, laminar bone; 5, Haversian bone. (B) Laminar bone from UALVP 60533. Scale bar = 500 µm. (C) Reticular bone from UALVP 60535. Scale bar = 500 µm. (D) Plexiform bone from UALVP 60535. Scale bar = 500 µm. (E) Haversian reconstruction from UALVP 60539. Scale bar = 500 µm.

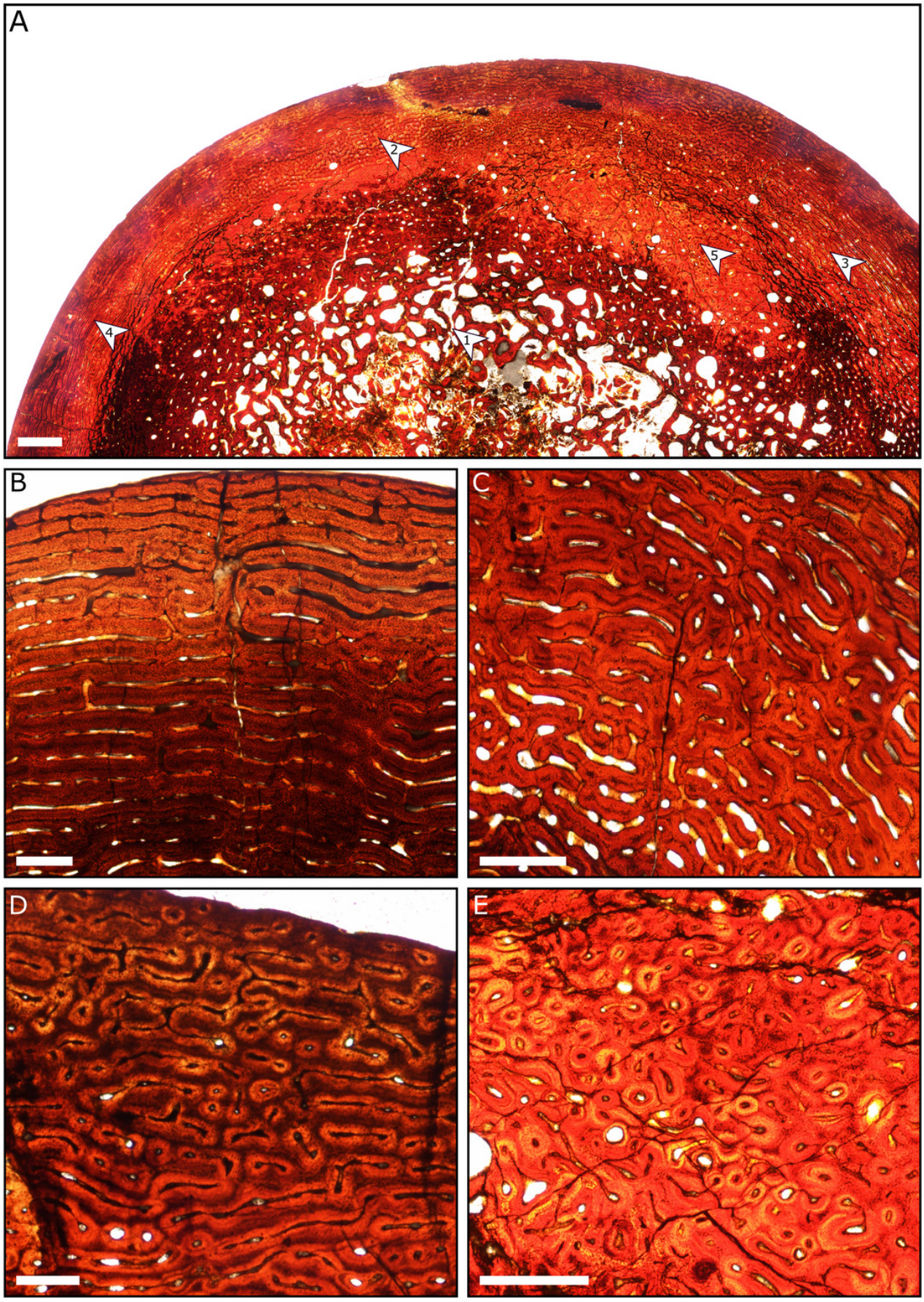
A
2
5
3
4
1
B
C
D
E

Figure 9

Distribution of bones at the Spring Creek Bonebed.

(A) The positively skewed size distribution of specimens from the bonebed. (B) A rose diagram of the recorded orientations of long bones from the Spring Creek Bonebed showing a preferential NE–SW modality, but overall high circular variance.

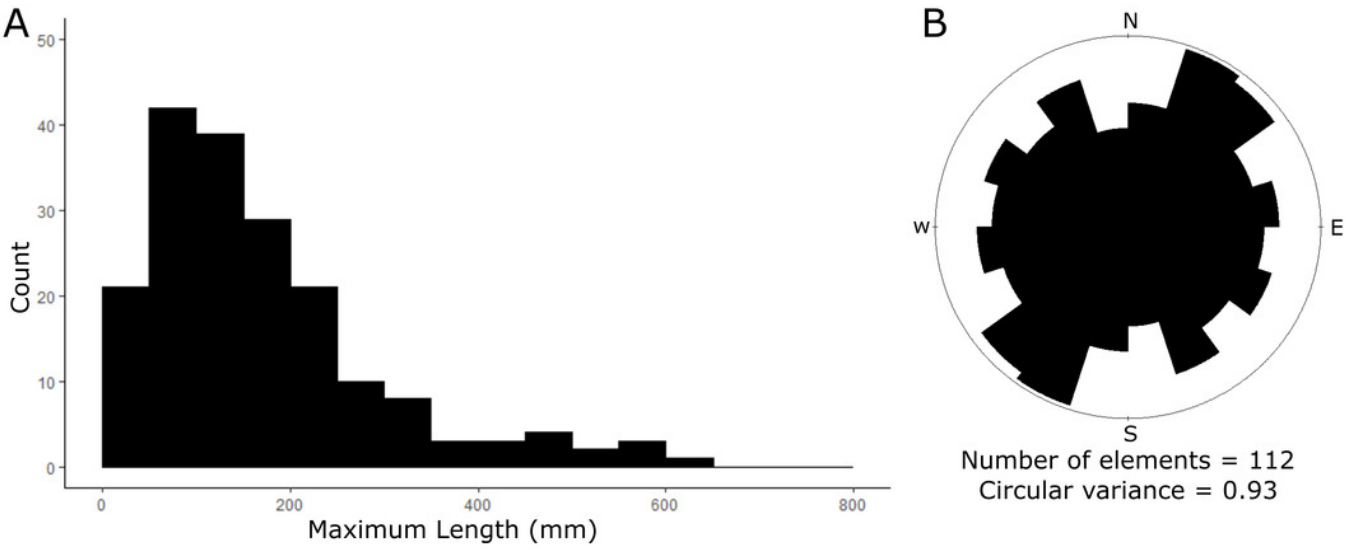

Figure 10

Examples of bone modification from the Spring Creek Bonebed.

(A) Unhealed parallel toothmarks (white arrows) on the lateral surface of the left dentary (UALVP 59907) interpreted as post mortem scavenging. (B) Pathology (margin indicated by white arrows) on the lateral surface of the supra-acetabular process (sa) from an incomplete ilium (UALVP 60540).

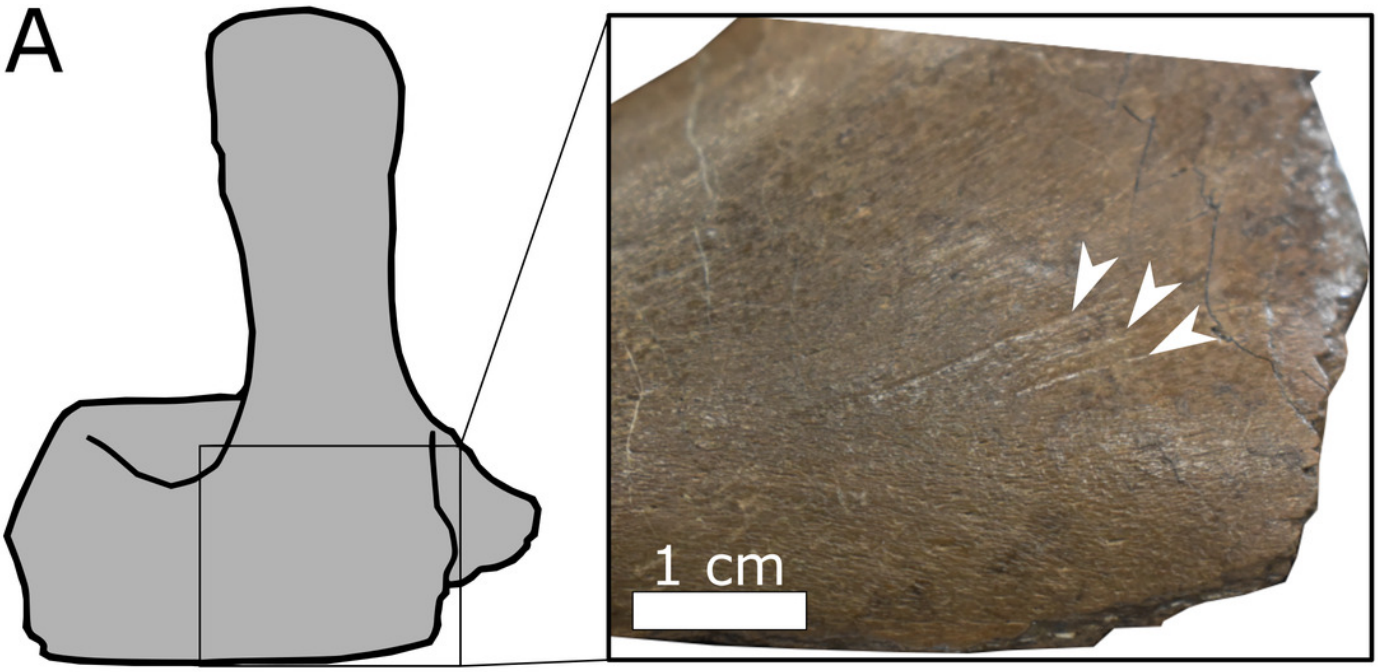
A
1 cm


B
sa
5 cm

Figure 11

Biostratigraphy and palaeobiogeography of temporally and spatially proximate Lambeosaurinae from Alberta, Canada, Montana, USA, and Mexico.

(A) Biostratigraphic distribution of Lambeosaurinae across strata from Montana, USA (Horner & Currie, 1994; Campbell et al., 2019), western and northeastern Mexico (Lucas & Sullivan, 2006; Gates et al., 2007; Prieto-Márquez et al., 2012; Fowler, 2017), and northwestern Alberta (Fanti & Catuneanu, 2009; this study), and southern Alberta, Canada (Mallon et al., 2012; Eberth et al., 2013; Eberth & Kamo, 2020). The Wapiti and Horseshoe Canyon formations are subdivided into units and members, respectively. Grey stratum represents the marine Bearpaw Formation (BPFm). The dashed range for the Spring Creek lambeosaurines represents a temporal range within Unit 3, between the Pipestone Creek Bonebed (73.5 Ma; (Currie et al., 2008b) and the basal most Horseshoe Canyon Formation (74.4 Ma; (Eberth & Braman, 2012). (B) Palaeobiogeographical distribution of Lambeosaurinae across Montana, USA, Alberta, Canada, and Mexico (Lull & Wright, 1942; Horner & Currie, 1994; Evans & Reisz, 2007; Evans et al., 2007; Gates et al., 2007; Evans et al., 2009; Evans, 2010; Prieto-Márquez et al., 2012). The silhouette of the Spring Creek lambeosaurine and *Magnapaulia laticaudus* were created by Scott Hartman and Dmitry Bogdanov, respectively. Both were vectorized by T. Michael Keesey and used under the creative commons attribution 3.0 unported license (https://creativecommons.org/licenses/by/3.0/). The remaining silhouettes were used and modified under the public domain dedication 1.0 license.

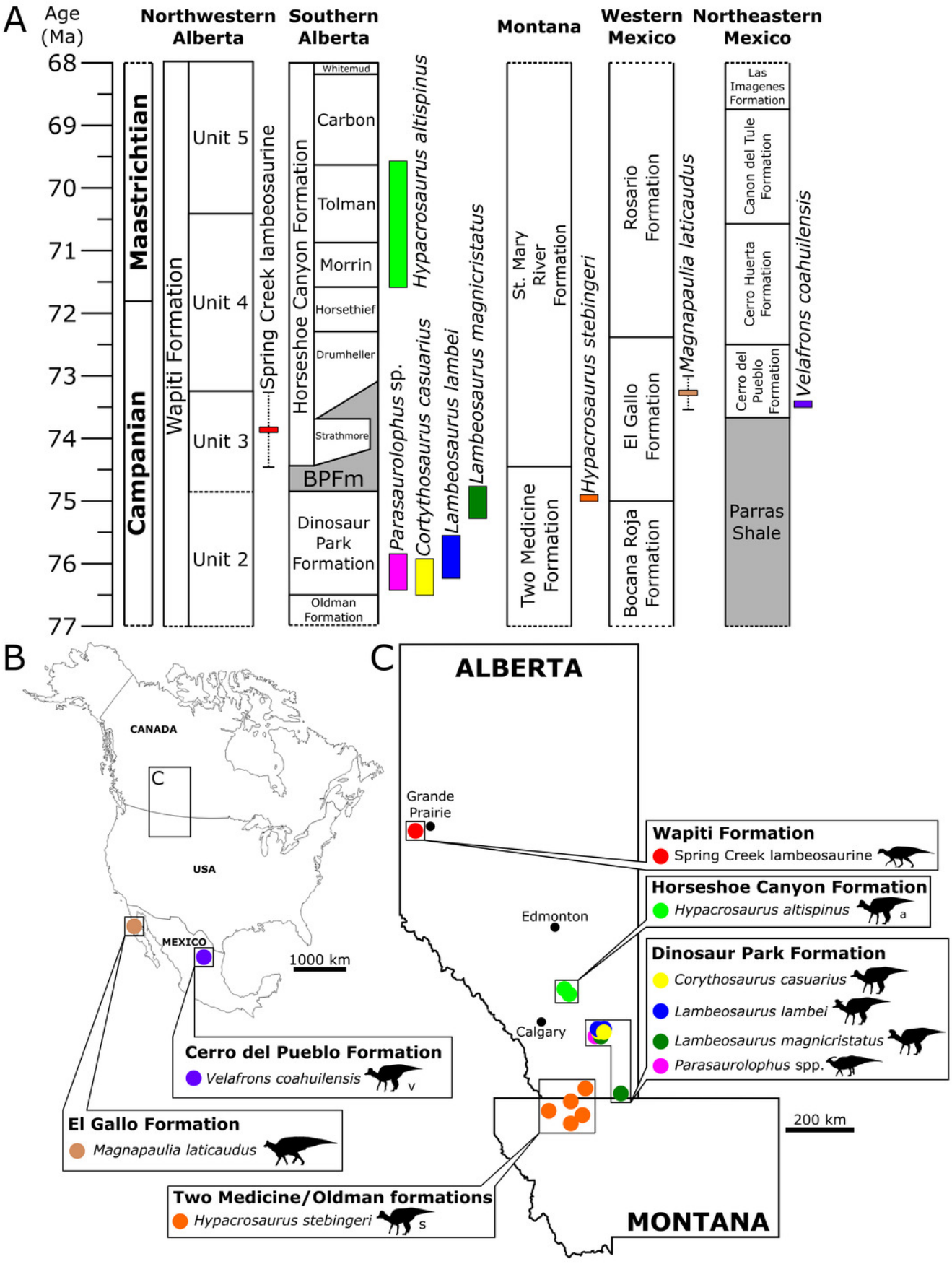
A
Age (Ma)
Northwestern Alberta
Southern Alberta
Montana
Western Mexico
Northeastern Mexico
68
69
70
71
72
73
74
75
76
77
Maastrichtian
Campanian
Wapiti Formation
Unit 5
Unit 4
Unit 3
Unit 2
Spring Creek lambeosaurine
Horseshoe Canyon Formation
Whitemud
Carbon
Tolman
Morrin
Horsethief
Drumheller
Strathmore
BPFm
Dinosaur Park Formation
Oldman Formation
Hypacrosaurus altispinus
Parasaurolophus sp.
Corythosaurus casuarius
Lambeosaurus lambei
Lambeosaurus magnicristatus
St. Mary River Formation
Two Medicine Formation
Hypacrosaurus stebingeri
Rosario Formation
El Gallo Formation
Bocana Roja Formation
Magnapaulia laticaudus
Las Imagenes Formation
Canon del Tule Formation
Cerro Huerta Formation
Cerro del Pueblo Formation
Parras Shale
Velafrons coahuilensis
B
CANADA
USA
MEXICO
C
1000 km
C
ALBERTA
Grande Prairie
Edmonton
Calgary
Wapiti Formation
Spring Creek lambeosaurine
Horseshoe Canyon Formation
Hypacrosaurus altispinus
a
Dinosaur Park Formation
Corythosaurus casuarius
Lambeosaurus lambei
Lambeosaurus magnicristatus
Parasaurolophus spp.
Cerro del Pueblo Formation
Velafrons coahuilensis
v
El Gallo Formation
Magnapaulia laticaudus
Two Medicine/Oldman formations
Hypacrosaurus stebingeri
s
200 km
MONTANA